



MINISTRY OF EDUCATION AND RESEARCH

National University of Science and Technology POLYTECHNIC
BUCHAREST

Doctoral School of
Industrial Engineering and Robotics

No. CSUD decision 07 from 06.03.2024

DOCTORAL THESIS

- ABSTRACT -

Gear modelling and power loss study in a mechanical transmission with helical gears

Ph.D. candidate: Alexandru-Adrian V. ILIEȘ

Thesis supervisor: Prof. dr. eng. Sorin CĂNĂNĂU

DOCTORAL COMMITTEE

President	Prof. dr. eng. Liviu-Daniel GHICULESCU	from	National University of Science and Technology Polytechnic Bucharest
Doctoral supervisor	Prof. dr. eng. Sorin CĂNĂNĂU	from	National University of Science and Technology Polytechnic Bucharest
Reviewer	Prof. dr. eng. Lorena DELEANU	from	University „Dunărea de Jos” of Galați
Reviewer	Prof. dr. eng. Simion HARAGĂȘ	from	Technical University of Cluj-Napoca
Reviewer	Prof. dr. eng. Alexandru Valentin Rădulescu	from	National University of Science and Technology Polytechnic Bucharest

Bucharest

- 2024 -

Contents

Introduction.....	4
List of abbreviations and symbols	4
Chapter 1. Current status of experimental research on helical gears.....	6
1.1. The history and evolution of gearboxes	6
1.2. Gear test rigs	7
1.2.1. Types of gear testing rigs.....	7
1.2.2. The current status of experimental research.....	9
1.3. Conclusions.....	10
Chapter 2. 2D and 3D numerical modelling of external cylindrical gears with inclined tooth and involute profile. Numerical developments.	10
2.1. Introduction.....	10
2.2. Geometrical elements of the gear used.....	10
2.3. Geometric modelling of gearing and gear wheels using numerical methods.....	10
2.4. The comparison between the involute profile created in NX and SE with the profile from the software libraries	10
2.5. Comparison of position and diameter differences between designed and imported wheels from the library.....	10
2.6. Conclusions.....	11
Chapter 3. Methodology for research and development of power losses in a mechanical transmission with cylindrical toothed gears and helical gears	12
3.1. Research and development directions.....	12
3.2. The main objective of the research and development activity	12
3.3. Research and development methodology.....	12
Chapter 4. Power losses in a mechanical transmission with cylindrical gears and helical teeth.....	12
4.1. Introduction.....	12
4.2. Thermal network	13
4.2.1. Transfer to the thermal network.....	13
4.3. Power losses in a mechanical transmission.....	13
4.3.1. Rheological experimental investigations on the behaviour of the oil used in the test rig	14
4.3.2. Friction losses due to gear meshing.....	14

4.3.3. The calculation of power loss in bearings	17
4.3.4. Power loss at the contact between the shaft and the seal.....	19
4.3.5. Power loss caused by oil churning in the gearbox.....	20
4.3.6. The total power lost in the transmission	23
Chapter 5. Experimental analysis. Evaluation of power losses in mechanical gear transmissions. ...	25
5.1. Introduction.....	25
5.2. Test rig presentation	25
5.3. Testing procedure	27
5.4. Results of the tests.....	28
5.5. Establishing the dependence of power dissipated through the housing on the temperature difference between the oil bath and the ambient environment.....	32
Chapter 6. Final conclusions and main contributions to power losses analysis in a thermal network with mechanical transmission and the experimental part: assessment of power losses in gear mechanisms.....	36
6.1. General conclusions	36
6.2. Original contributions of the doctoral thesis	37
Selective bibliography.....	38

Introduction

The doctoral thesis focuses on the investigation of helical cylindrical gear systems in the field of mechanical engineering, addressing experimental aspects, numerical modeling, and theoretical and experimental analysis of power losses in mechanical transmissions with such gears. The study makes significant contributions through advancements in experimental research, the development of specialized test rigs, and 2D and 3D numerical models for evaluating gear behavior. Additionally, special attention is given to the theoretical analysis of power losses. By integrating theoretical and experimental information, the thesis aims to contribute to the understanding and optimization of the performance of helical cylindrical gears with inclined teeth.

List of abbreviations and symbols

No.	Abbrev.	Significance
01	b	Tooth width
02	C_m	Torque moment load factor
03	$d_{1,2}$	Pitch diameter of pinion, driven gear
04	ε	Gear tooth coverage
05	η	Lubricant viscosity
06	H	Oil level
07	H_v	Geometry parameter
08	L_0	Depth of immersion of the driven gear in the oil bath
09	m	Temperature parameter
10	M	Total bearing friction moment
11	m_n	Normal module of the tooth
12	M_0	Total friction moment in load-independent losses
13	M_1	Total friction moment in load-dependent losses
14	Mt	Transmitted moment
15	n	Rotation speed / Flow index
16	P_{churn}	Power loss due to oil churning
17	P_{etansare}	Total sealing power loss

18	P_{in}	Power at the pinion
19	P_{mesh}	Power loss in meshing
20	P_{rulm}	Power loss in a bearing
21	P_v	Lost power
22	Q	Heat flux
23	Q_{cond}	Heat dissipated through conduction
24	Q_{conv}	Heat dissipated through convection
25	Q_{diss}	Heat dissipated
26	Q_{rad}	Heat dissipated through radiation
27	R	Thermal resistance of the conductor in the thermal network model
28	R_{term}	Thermal resistance
29	T	Temperature
30	T_{oil}	Oil temperature
31	t	Time / Angle belonging to the interval [0;1]
32	T_{wall}	Transmission housing temperature
33	ω	Angular velocity
34	W_L	Specific load
35	x	Profile radial displacement coefficient
36	X_C	Correction factor for cemented gears
37	X_L	Lubricant correction factor
38	z	Number of teeth on the gear
39	β	Tooth inclination angle on the pitch cylinder
40	ΔT	Temperature difference between the equilibrium temperature in the oil bath and the ambient temperature
41	η	Dynamic viscosity of the lubricant
42	μ	Friction coefficient

Chapter 1. Current status of experimental research on helical gears

1.1. The history and evolution of gearboxes

The history of gears is presented, starting with their use in antiquity, including ancient Egypt, Greece and Rome. Figure 1.1, a primitive wooden gear, exemplifies their application in those remote periods.

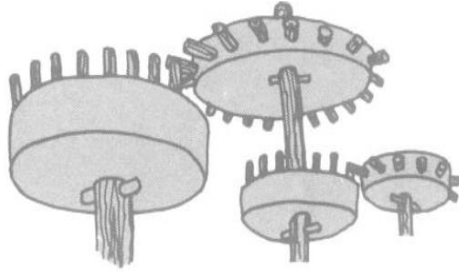


Fig. 1.1 Primitive wooden gearbox [1]

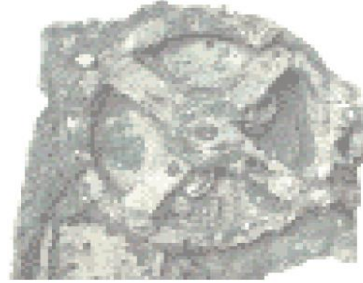


Fig. 1.2 The Antikythera mechanism [2]

Mention is made of the advanced culture of Ancient Greece, where gear systems with toothed wheels were present as early as 1900 BC, illustrated by Figure 1.2 - The Antikythera mechanism used for astronomical calculations.

The important contributions of thinkers such as Aristotle and Archimedes are highlighted, including the description of the rolling motion of two tangent circles and the introduction of the concept of the snail-wheel mechanism, illustrated by Figure 1.3 - The Southern pointing chariot.



Fig. 1.3. The Southern pointing chariot.
Model made by George H. Lanchester. Science Museum in
London [5]

The transition to the Renaissance period brings into question the diversity of gear mechanisms designed by Leonardo da Vinci (Figure 1.4 - Helical gear - Codex Atlanticus). The importance of these historical periods in the development of gears and gear mechanisms is highlighted.

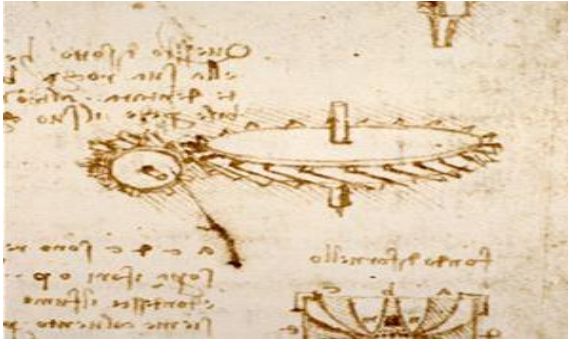


Fig. 1.4. Helical gearing - Codex Atlanticus [7]

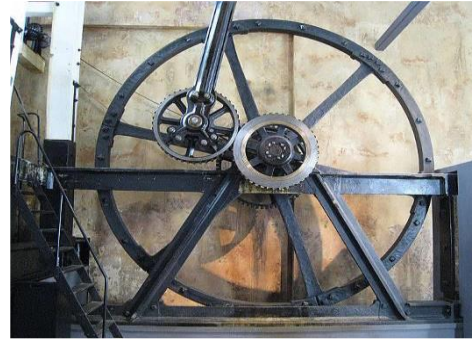


Fig. 1.5. Planetary gear mechanism - James Watt [8]

The age of industrialisation is illustrated by the significant contributions of figures such as Christian Huygens and James Watt, who introduced innovations such as the pendulum regulator and the planetary gear (Figure 1.5 - Planetary gear mechanism - James Watt).

Throughout evolution, gears have played a crucial role in various fields, including the development of vehicles and machine tools. Gottlieb Daimler's innovations and advances in modern gearboxes have reinforced the importance of gears in mechanical transmissions.

In conclusion, sub-chapter 1.1, provides a detailed look at the history and evolution of gears, highlighting their importance in the transmission of rotary motion. From their earliest use in ancient human times to their integration into modern technology and biological structures, gears have played a key role in technical and scientific progress. The groundbreaking discovery of the gear mechanism in the biological world, illustrated in Figure 1.8 and 1.9, where the gear mechanism of the insect *Issus coleoptratus* is shown, suggests that the study of these mechanisms can inspire the development of efficient small-scale gears in biology.



Fig. 1.8. *Issus coleoptratus* insect [11]

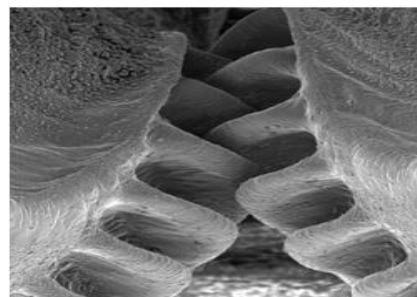


Fig. 1.9. Gear mechanism of the insect *Issus coleoptratus* [11]

1.2. Gear test rigs

In this sub-chapter, I focused on test rigs, used to evaluate the characteristics of the gears and the loading modes applied during the experiments. I will explore different types of rigs and loading modes, highlighting their specific advantages and uses in gear testing.

1.2.1. Types of gear testing rigs

In the specialized literature [12-23], the main types of gear testing rigs are described, as illustrated in Figure 1.16:

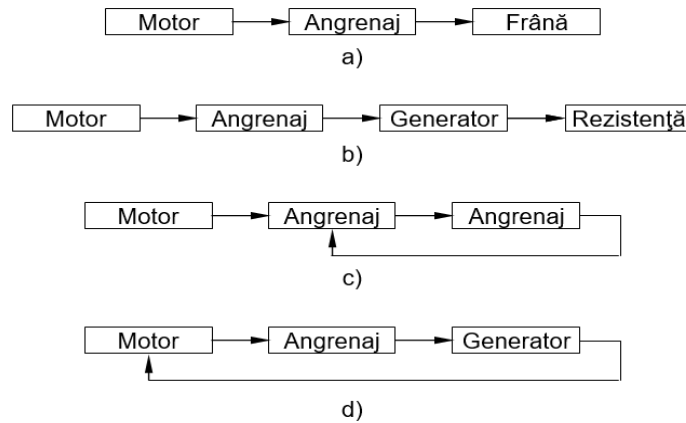


Fig. 1.16. Types of gear testing rigs: open mechanical circuit (a), open electrical circuit (b), closed mechanical circuit (c), closed electrical circuit (d).

The major difference between open circuit and closed circuit testing rigs lies in the fact that in open circuit rigs, the entire load power is lost, while in closed circuit rigs, the external power source only needs to compensate for frictional losses. These rigs, regardless of their type, ensure the loading of the gears under testing and are essential for evaluating their performance.

Loading in open circuit rigs is achieved through the use of a brake, as depicted in Figure 1.17, illustrating a simple mechanical loading system applied to the testing of spur gears. In Figure 1.18, the same principle is implemented, but the loading is done hydraulically, introducing improvements.

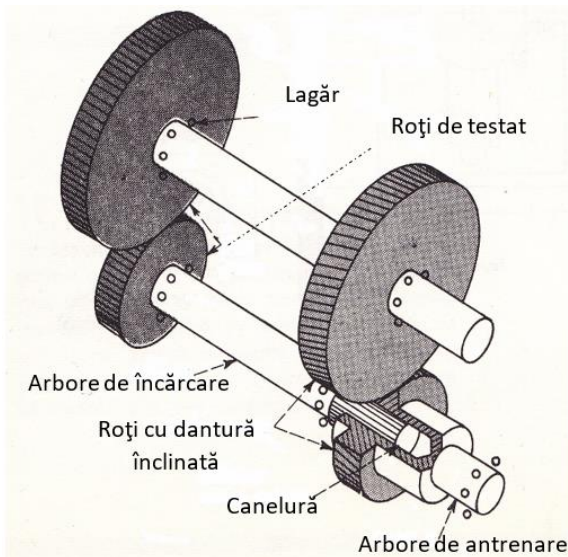


Fig. 1.17. Loading system for spur gears, closed-circuit rig (after Chironis, 1967). [12]

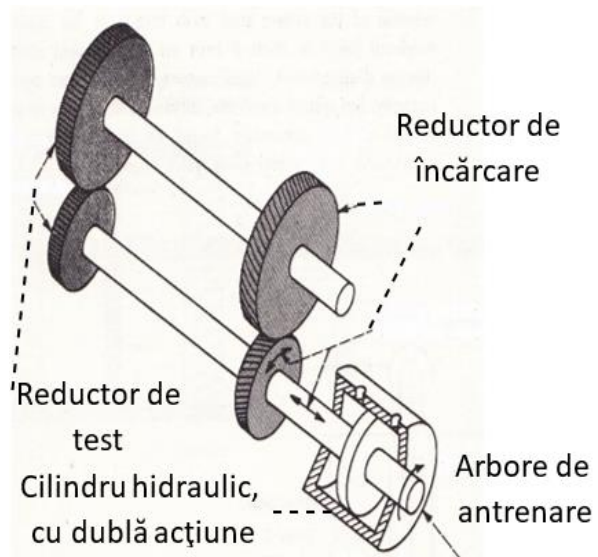


Fig. 1.18. Hydraulic loading system for spur gears, closed-circuit rig (after Chironis, 1967) [12]

1.2.2. The current status of experimental research

This section focuses on the importance and results of experimental research within the thesis, highlighting the closed-circuit FZG testing rigs and their significant contributions to understanding the behavior of gears in various operating scenarios.

Hargreaves and Planitz (2008) [13] provide a detailed description of the FZG-type gear testing rig in Figure 1.20, incorporating a power recirculation loop, suitable for a multitude of gear tests.

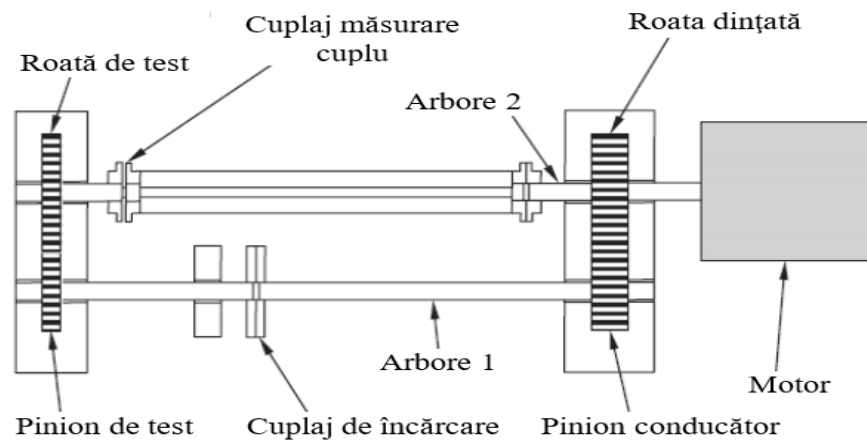


Fig. 1.20. Closed-circuit FZG gear testing rig, for the study of gears, (Hargreaves, Planitz, 2008) [13]

Li (2008) [14] uses closed-loop mechanical rigs to study torsional vibration phenomena in gear systems.

The rig designed in the framework of the European contract ESPOSA, WP 3.4., by INCDT - COMOTI, is intended for testing gears for pitting, scuffing and scoring [15], is shown in Figures 1.22 and 1.23.

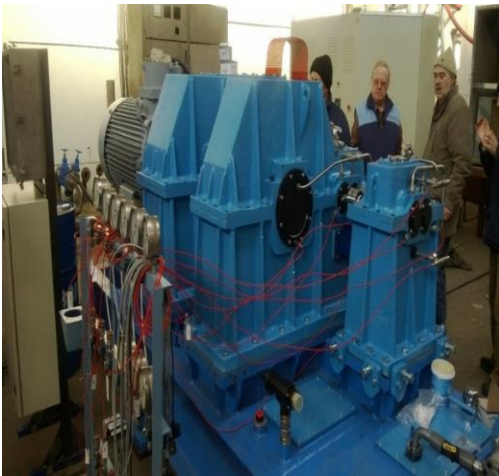


Fig. 1.22. Gear Testing Rig ESPOSA – INCDT-COMOTI, (after Gabroveanu, 2016) [15]

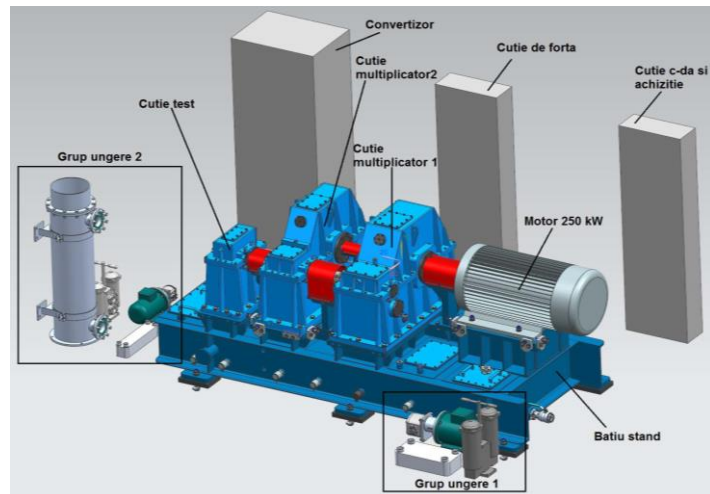


Fig. 1.23. Composition of the gear testing rig at INCDT-COMOTI (after Gabroveanu, 2016) [15]

Davali et al. (2007) [16] used a gear noise measurement rig to study the total gear error using optical encoders and elastic couplings.

Raja Hamzah and Mba (2008) [17] investigated the influence of operating conditions on the level of gear noise emission using a closed-circuit rig.

Tan and Mba (2004) [18] developed a diagnostic rig for identifying gear wear and accuracy using repeatable and reliable closed-circuit methods.

The study by Khang, Cau and Dien (2004) [19] investigated the vibration of gears by analyzing subharmonics as a diagnostic element using a closed-circuit rig.

1.3. Conclusions

An analysis of the history and evolution of gears reveals significant advances in technology, materials and manufacturing methods. Test rigs have become essential for evaluating gear performance in a controlled environment, ranging from simple to advanced rigs that allow testing under various load and lubrication conditions.

Current research in the field is aimed at improving test rigs to provide accurate and relevant results on gear behaviour and durability. This chapter highlights not only the complexity of research in this field, but also its importance in advancing technology and optimising the performance of gear drive systems.

Chapter 2. 2D and 3D numerical modelling of external cylindrical gears with inclined tooth and involute profile. Numerical developments.

2.1. Introduction

The diversification of manufacturing technologies for gears is noted, and the author proposes a comparison between involute profiles generated in Siemens Unigraphics NX 12 and Solid Edge ST9, utilizing Excel, and those from their respective libraries.

2.2. Geometrical elements of the gear used

Selected gear characteristics are given, including number of teeth, modulus, gear and pitch angles, axle spacing, tooth width, and radial displacement coefficients.

2.3. Geometric modelling of gearing and gear wheels using numerical methods

The methods for generating the involute profile in Siemens Unigraphics NX 12 and Solid Edge ST9 are described in detail. For each program, steps such as importing coordinates, generating 2D curves or profiles, and 3D modeling of gears are presented.

2.4. The comparison between the involute profile created in NX and SE with the profile from the software libraries

A detailed comparison is conducted between the involute profiles modeled in Siemens Unigraphics NX 12 and Solid Edge ST9 and those from the software libraries. Angles, diameters, and phase differences are analyzed to assess the accuracy and correspondence between the profiles created by the author and the standard profiles from the libraries.

2.5. Comparison of position and diameter differences between designed and imported wheels from the library

Following the analysis of the wheels designed and imported from the library, we observed differences in the position of the homologous points, i.e. for the same angular position on the flank, small differences in diameter are observed.

To visualize the differences between the profiles modelled in the 2 programs, we superimposed them as in Fig. 2.40. The zoom is made in the area of the splitting diameter, this is magnified about 1550 times to be able to observe the deviation of the order of 10^{-5} mm. In Fig. 2.41, an area of profile has been chosen for highlighting, where the maximum difference between the profile modelled in NX and the profile modelled in SE is observed.

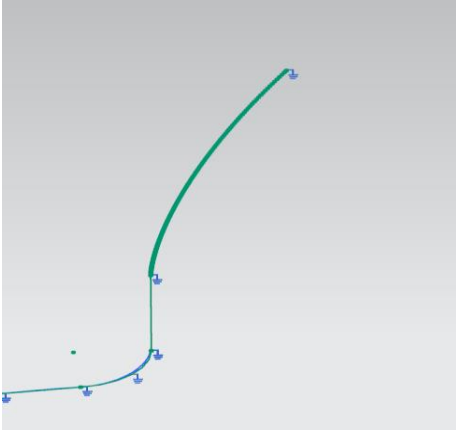


Fig. 2.40. Profile overlap

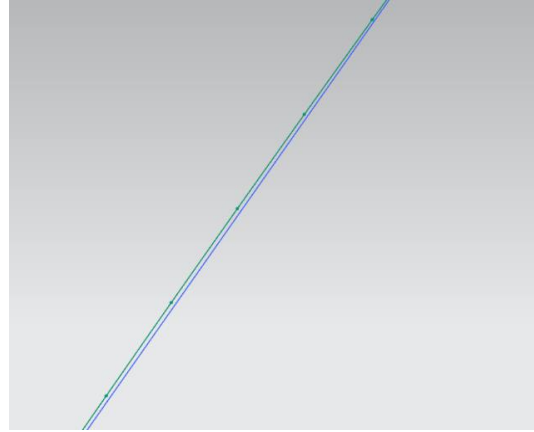


Fig. 2.41. Overlap of profiles at Scale [1550:1]

The profile differences highlighted above were due to accuracy error in program design and differences in the program used to import the point set.

Based on this information, the geometry required to build the gears to be integrated into the test rig will be developed.

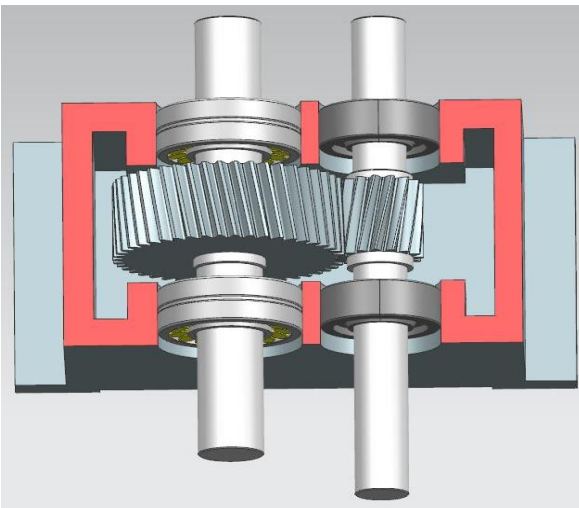


Fig. 2.42. 3D gearing made in Siemens Unigraphics NX 12



Fig. 2.43. Lower half housing, with mounted gearing, made at Cugir Mechanical Plant

2.6. Conclusions

Finally, section 2.6 draws important conclusions. The involute profile generation process in Siemens Unigraphics NX 12 is described as facilitating the accurate modelling of gears, providing

advanced options and tools for adjusting and optimising the tooth shape. Solid Edge ST9 also provides facilities for involute profile generation, helping to develop and optimise gears.

Comparison between the two software shows satisfactory results, with some subtle differences. The detailed findings represent a significant contribution to existing knowledge and provide a solid basis for further research and development in the modelling of helical gears.

Chapter 3. Methodology for research and development of power losses in a mechanical transmission with cylindrical toothed gears and helical gears

Chapter 3 explores the research and development methodology of power losses in mechanical gear transmissions with cylindrical gear and helical teeth.

3.1. Research and development directions

- Identify the main sources of power loss.
- Assessment and quantification of specific losses.
- Optimisation of gear design and geometry.
- Investigation of the influence of lubrication and sealing on losses.

3.2. The main objective of the research and development activity

Establishing and validating innovative solutions for theoretical and experimental power loss analysis to improve the efficiency of mechanical transmissions.

3.3. Research and development methodology

- Literature review to understand previous research.
- Identify the relevant components for losses.
- Design and construction of an experimental device.
- Conduct experimental tests and record data.
- Analysis and interpretation of experimental results.
- Development and evaluation of design optimization methods.
- Comparison of experimental results with analytical models and numerical simulations.
- Documenting results and writing the PhD thesis.

This methodology aims to gain a comprehensive understanding of power losses in gear drives, contributing to the development of efficient and sustainable solutions.

Chapter 4. Power losses in a mechanical transmission with cylindrical gears and helical teeth

4.1. Introduction

Modern gear drive design aims to improve the energy properties of new products. The study focuses on the detailed assessment of energy losses in a gear transmission system, thermally converted to heat. The authors investigated thermal patterns, thermal load differences of cylindrical gears, thermal processes in gears and lubricant behaviour, thus contributing to optimising the efficiency of gear systems.

4.2. Thermal network

A thermal network model used to estimate power losses in gear transmissions is presented. The authors discuss existing methods and analogies between electrical and thermal networks. The sources of thermal resistance are highlighted and the structure of power losses in a mechanical transmission is detailed. The working model of such a unit is shown in Figure 4.1.

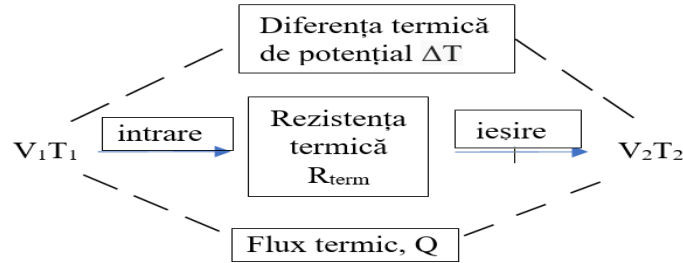


Fig. 4.1. Thermal network model

4.2.1. Transfer to the thermal network

Sources of thermal resistance and thermal equilibrium in the mechanical system are examined. The authors stress the importance of correlating power loss with heat energy discharge and describe heat transfer mechanisms such as convection, radiation and conduction. A method of calculating the total heat dissipated is proposed, and the problem of determining the value of the heat transfer coefficient is discussed in detail.

In Figure 4.2, the main components responsible for power losses in a mechanical transmission are highlighted.

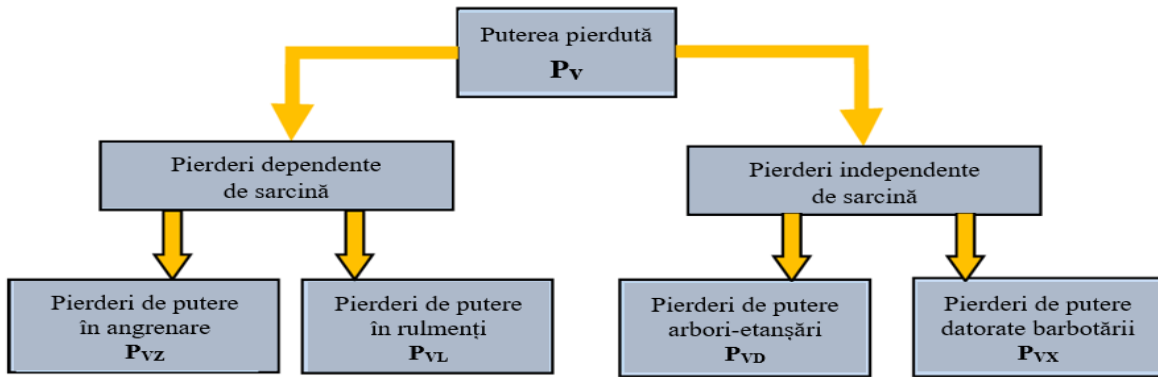


Fig. 4.2. The structure of power losses in a mechanical transmission. [57]

According to [56], it can be written:

$$P_V = P_{VZ} + P_{VL} + P_{VD} + P_{VX} \quad (4.2)$$

4.3. Power losses in a mechanical transmission

Heat dissipation Q_{dis} is a summation of the heat removed by conduction ($\sum_{j=1}^m \dot{Q}_{j,cond}$), convection ($\sum_{i=1}^n \dot{Q}_{i,conv}$) and radiation ($\sum_{k=1}^p \dot{Q}_{k,rad}$), for all system components that, over time, are assumed to be in the process of dissipating.

$$\dot{Q}_{dis} = P_V \quad (4.7)$$

$$\dot{Q}_{dis} = \sum_{i=1}^n \dot{Q}_{i,conv} + \sum_{j=1}^m \dot{Q}_{j,cond} + \sum_{k=1}^p \dot{Q}_{k,rad} \quad (4.8)$$

4.3.1. Rheological experimental investigations on the behaviour of the oil used in the test rig

In sub-chapter 4.3.1, experimental rheological investigations were carried out on the behaviour of H46EP oil used in the test rig. The viscosity properties of the lubricant were examined and several expressions were used for the viscosity versus temperature relationship, including the power law model. Experiments were carried out to investigate the rheological behaviour of the oil under various operating conditions.

To evaluate the rheology of oil, comparative rheograms were carried out, analysing the variation of tangential stresses as a function of velocity gradient and the variation of viscosity as a function of temperature. Rheological parameters such as consistency index (m) and flow index (n) were identified for fresh and used oil using the power law model. The experimental values were compared with the theoretical curves calculated using the Reynolds model and the results were considered satisfactory for use in subsequent theoretical calculations.

4.3.2. Friction losses due to gear meshing

Subchapter 4.3.2 focuses on friction losses in gear transmission. A detailed calculation of these losses under mixed lubrication conditions, where the normal tooth contact load is not fully supported by the EHD lubricant film, is outlined. In actual operation, there are variations in the thickness of the lubricating film due to different moments in the gearing as well as uneven load distribution. This issue is addressed in the analysis by adopting a computational model proposed by Fernandez and co-workers [60], which is detailed and modified.

$$P_{mesh} = \mu_{fz} \cdot P_{in} \cdot H_v \quad (4.21)$$

where P_{mesh} is obviously the gearing power loss, μ_{fz} is the gearing friction coefficient, P_{in} is the power at the pinion shaft (of the driving wheel), H_v is a geometry parameter described in the same paper [60]:

$$H_v = \frac{\pi(u+1)}{z_1 \cdot u \cdot \cos\beta_b} (1 - \varepsilon) \quad (4.22)$$

where u is the transmission ratio, z_1 number of teeth of the drive wheel, β is the angle (helix) of inclination of the teeth, ε is the gear tooth coverage.

The University of Porto team, led by Seabra, introduces an important aspect of the influence of surface quality on the coefficient of friction in meshing. They propose a new calculation model developed by Castro and Seabra [71]:

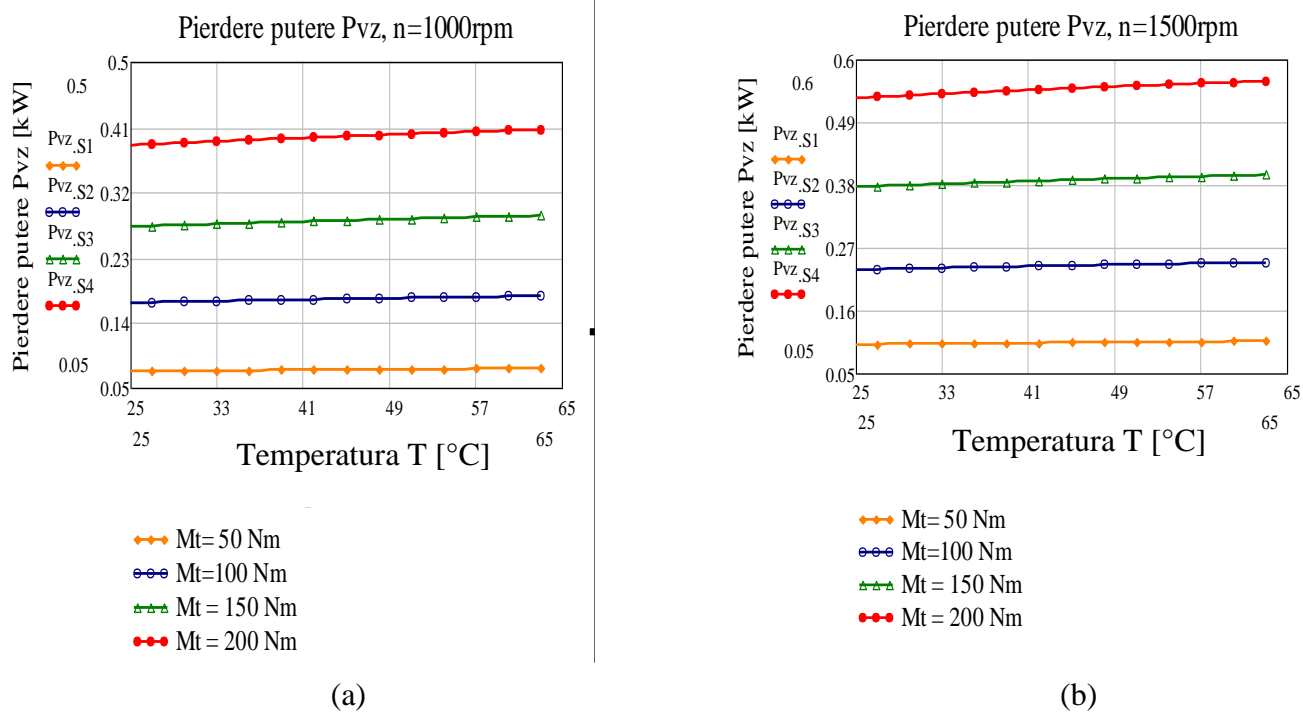
$$\mu_{fz} = 0,171 \left(\frac{W_L}{R'_{eq(C)} \cdot V_R} \right)^{0,2} \eta^{-0,05} \left(\frac{Ra_{Eq}}{d_1} \right) X_L X_C \quad (4.27)$$

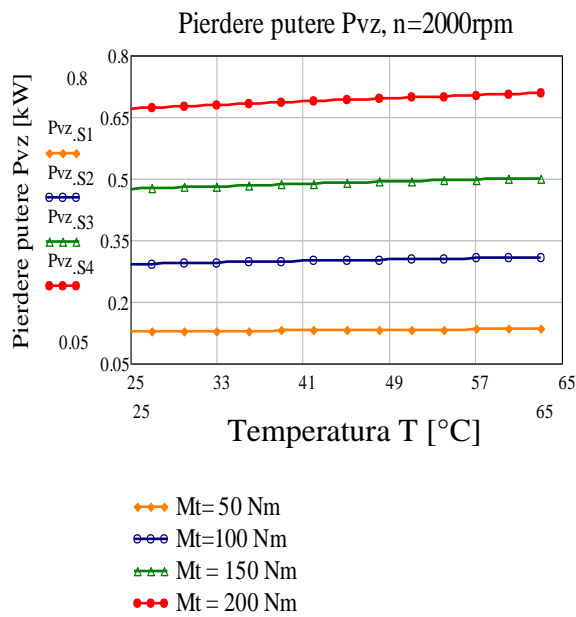
where W_L is the specific load, V_R is the rolling velocity (velocity at point C of the meshing), $R'_{eq(C)}$ is the equivalent radius of curvature at the point of contact (C), η is the dynamic viscosity of the oil at operating temperature, d_1 is the pinion pitch diameter, Ra_{Eq} is the arithmetic mean of the surface roughnesses in contact, X_L is the lubricant correction factor, and is a function of the nature

of the additive used in the oil, and X_C is the correction factor for cemented gears (since the gears in the stand are hardened the value $X_C=1$ has been adopted).

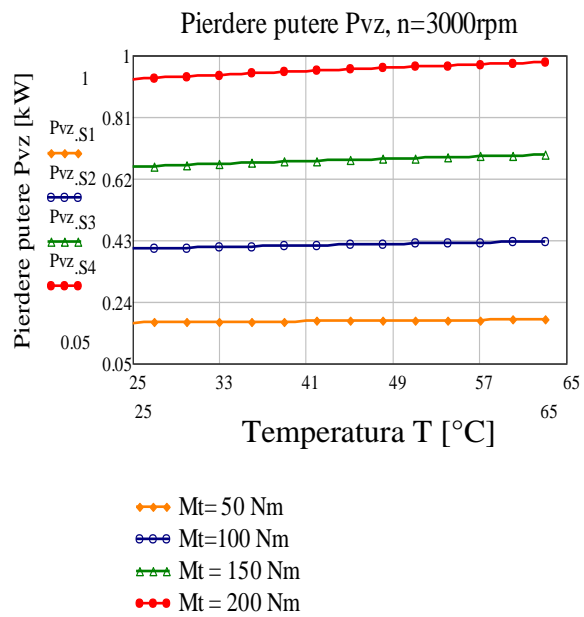
This relationship is used in the analysis presented in the thesis, considering it complete in terms of the influence of load, material, contact surface and lubricant properties. The results of this analysis are integrated into equation (4.21) for the calculation of the power losses in meshing, with the factors specified in relation (4.22).

Analysis of the results indicates gear power losses in the order of several hundred watts, ranging from 100 to 1000 watts, depending on speed and load. These losses increase with speed and obviously with load. Figure 4.10 illustrates this relationship between power losses, speed and lubricant temperature. It can be seen that power loss values increase with speed and load.





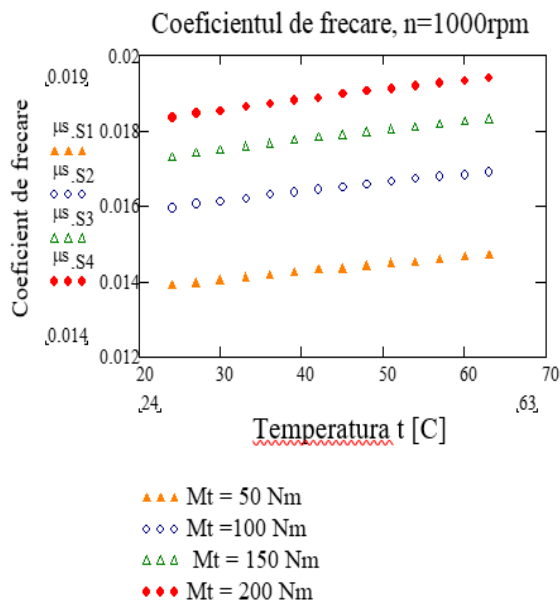
(c)



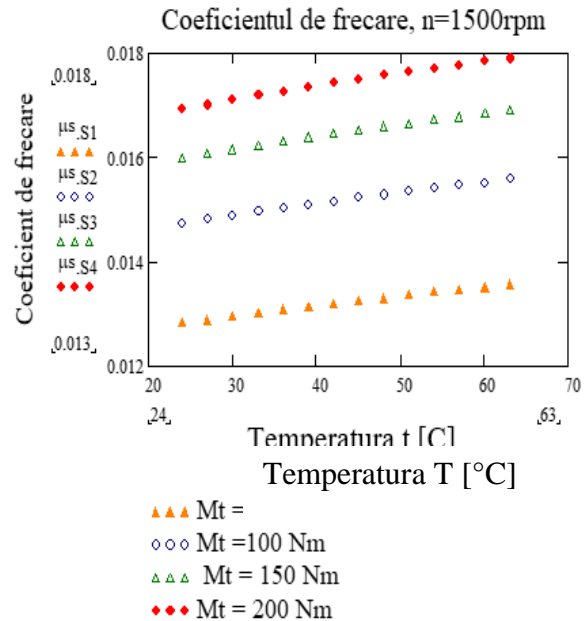
(d)

Fig. 4.10. Power losses in Pvz gearing in relation to speed and lubricant temperature

The explanation for these power losses is related to the increase in the coefficient of friction in gearing, shown in Figure 4.11. The coefficient of friction increases with speed and temperature, with a high dependence on load.



(a)



(b)

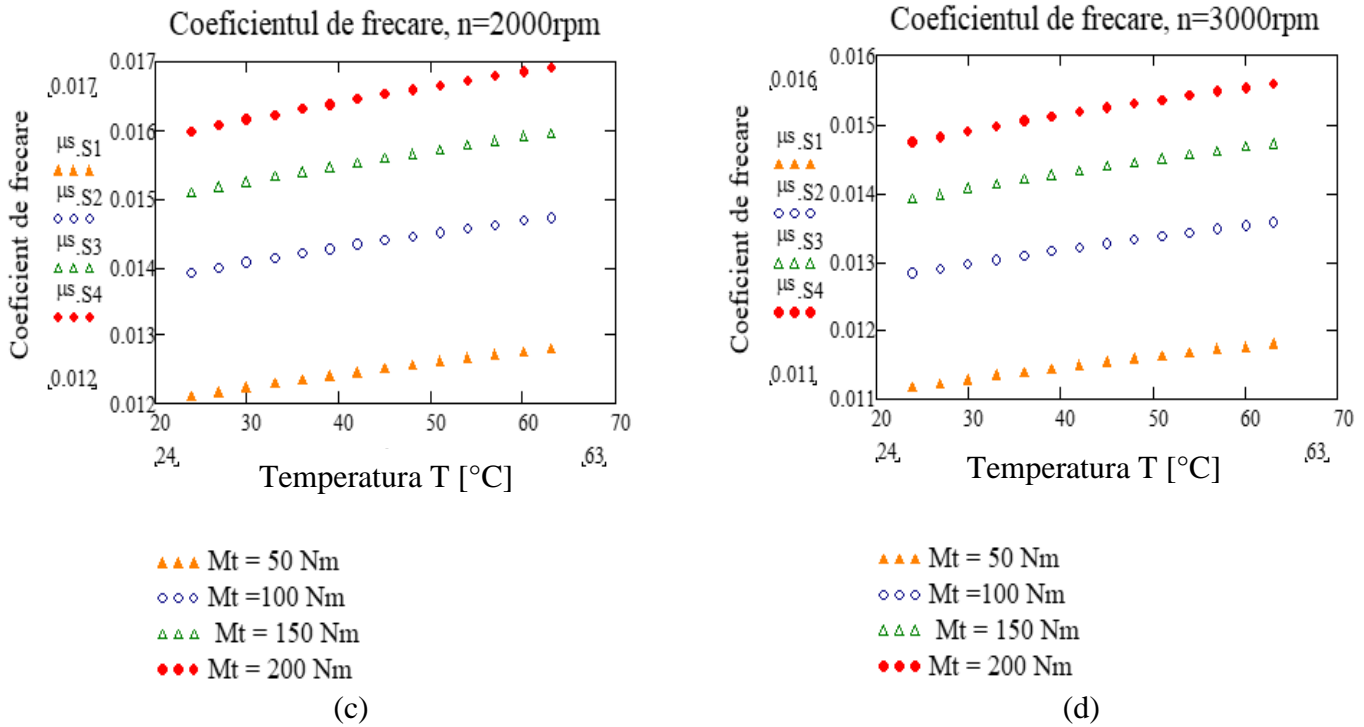


Fig. 4.11. Coefficient of friction μ , in gear, in relation to speed n

These results contribute to a deeper understanding of gear power losses and the influences of critical variables such as speed, load and lubricant temperature.

4.3.3. The calculation of power loss in bearings

In my power loss calculation process in bearings, I have carefully implemented the procedure recommended by SKF in 2004. The SKF model provides a detailed approach covering four main sources of moment losses in a rolling bearing: rolling friction moment (M_{rr}), sliding friction moment (M_{sl}), sealing friction moment (M_{seal}), and drag losses moment due to resistance, agitation, lubricant splash, etc. (M_{drag}).

By applying this procedure, I have ensured a precise assessment of power losses in bearings, integrating all significant sources contributing to heat generation in the bearings. The relation used is [89]:

$$M = M_{rr} + M_{sl} + M_{seal} + M_{drag} \quad (4.33)$$

The power loss in a bearing due to bearing friction can be estimated using [89].

$$P_{rulm} = M \cdot \omega = 1,05 \times 10^{-4} M \cdot n \quad (4.49)$$

P_{rulm} - power loss [W],

M - total bearing friction torque [Nmm],

n - rotational speed [rpm].

In this analysis, the focus was on studying the behaviour of the transmission system, with particular emphasis on the power lost in the bearings. The data shown in Figure 4.19 illustrates how power loss in the bearings is influenced by variations in speed, moment and temperature.

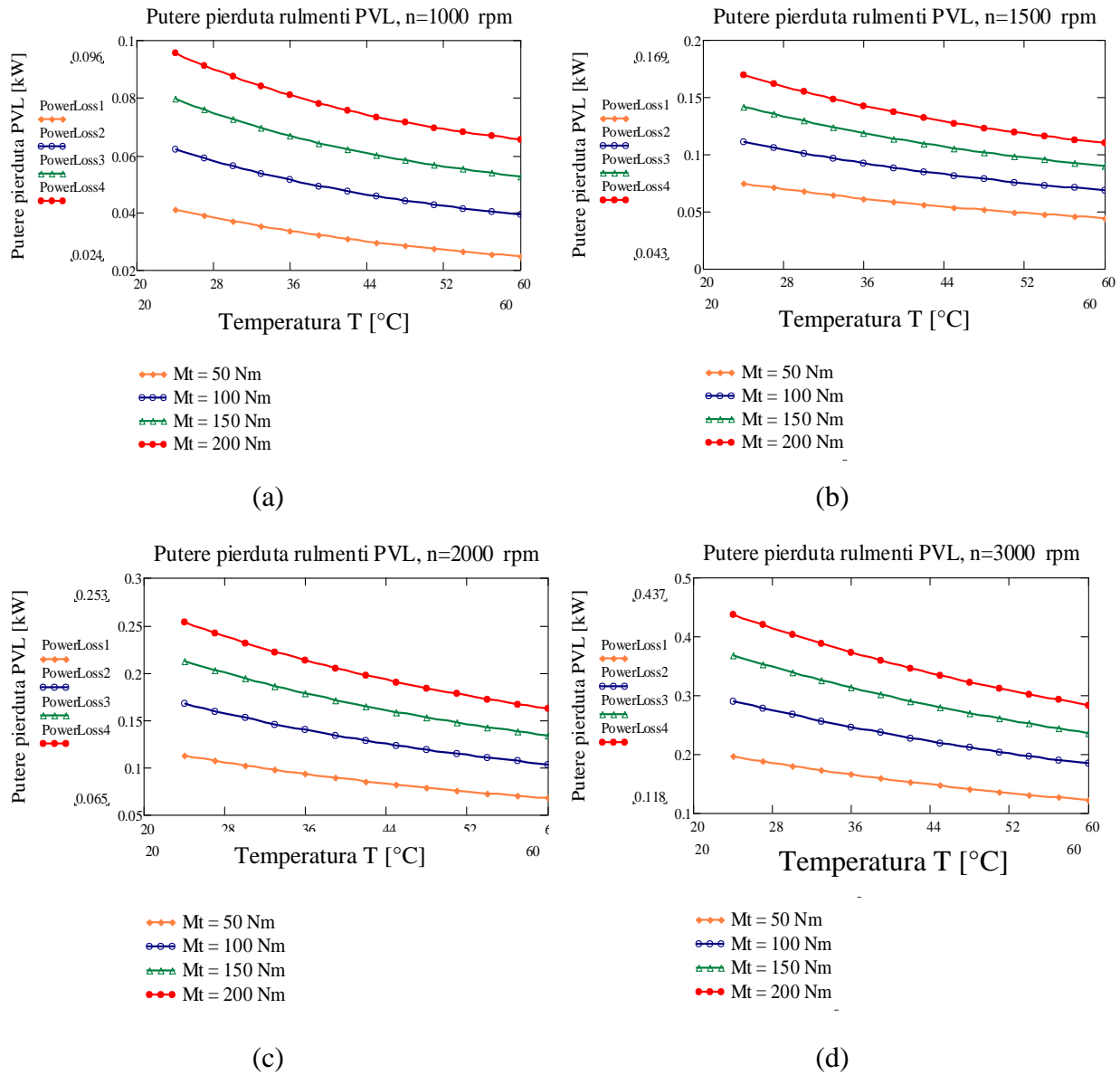


Fig. 4.19 Power losses in bearings, P_{VL} , in relation to speed and moment considered at transmission input (calculated values)

From the evaluation of the data presented in Figure 4.19, several significant conclusions can be drawn. The power lost through the bearings is indeed significantly influenced by these variables. First, we observed that the power lost in the bearings increases with increasing speed. The higher the speed, the more significant the power lost in the bearings becomes. Also, the applied torque has a significant influence on the power lost in the bearings, and this phenomenon is observed especially at high torque values.

Contrary to initial expectations, it is observed that the power lost in the bearings decreases with increasing temperature. This could be caused by changes in the properties of the lubrication

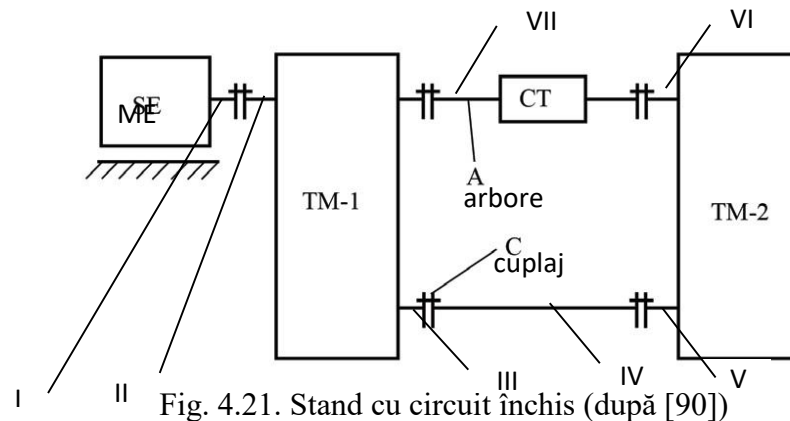
oil at higher temperatures, which may reduce the friction coefficient in the bearings and hence the power lost in the bearings..

The results indicate that special attention must be given to speed and momentum in the design and operation of the system to minimise power losses. The influence of temperature on the friction coefficient and therefore on the power lost in the bearings must also be considered..

4.3.4. Power loss at the contact between the shaft and the seal

Power loss due to friction between drive shafts and seals occurs in the stand we used for the experimental part of this study at the places where the shafts come out of the housing and form motion and load transmission links via couplings etc. This can be seen on the schematic diagram of the FZG stand used.

Shaft power loss - sealing is a part of the load-independent power loss, i.e. independent of the value of the transmitting moment. It is, however, dependent on the properties of the lubricant, which, like viscosity, are themselves temperature dependent, as well as on the value of the angular velocity, i.e. the speed of the drive shafts. As can be seen, there are five points of power loss in the shaft seal subsystem.



where

ME - is the electric motor,

TM-1 it's the first transmission,

TM-2 it's the second transmission,

CT - is the torque translator.

Power loss in the shaft-sealing system is also a controversial topic in the literature. However, both theoretical and experimental studies exist. In this study I will adopt the computational model presented by Jelaska [91]:

$$P_{etansare} = (145 - 1,6 \cdot T_{ulei} + 350 \cdot (\log(\log(v_{40} + 0.8)))) \cdot d_{(II,III,V,VI)}^2 \cdot n_{(II,III,V,VI)} \cdot 10^{-7} \quad (4.53)$$

In this relation the power for each shaft-seal contact is identified and calculated at shaft level II,III,V,VI by entering the diameter of the corresponding shaft in the seal and the shaft speed. The total power lost in the seal shall be calculated by summing the power lost locally in each seal.

As can be seen from the following figure (Fig. 4.22), the total power loss in sealing is not significant compared to the power lost through meshing, the power lost in the bearings and the power lost through churning. Also, the almost linear variation of the increase in lost power with increasing angular velocity, i.e. speed, n [rpm] is observed.

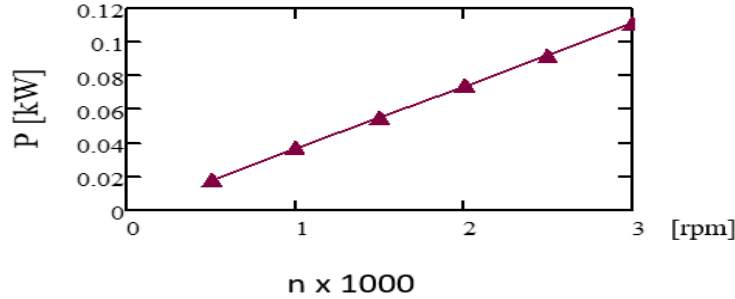


Fig. 4.22. Power loss in P_{VD} seals in relation to the shaft speed n

4.3.5. Power loss caused by oil churning in the gearbox

The power loss caused by oil churning is part of the load-independent power loss, i.e. independent of the value of the torque. It is also dependent on the properties of the lubricant, which, like viscosity, are themselves temperature dependent, as well as on the value of the angular velocity, i.e. the speed of the transmission shafts.

The equation that I will adopt in the current study is that given by Changenet et al [94],

$$P_{churn} = \frac{1}{4} (d_2 \cdot \omega)^3 \cdot \rho \cdot A \cdot C_m \quad (4.54)$$

where d_2 is the pitch diameter of the driven gear immersed in lubricant, ω is the angular velocity, ρ is the oil density, A is the lateral surface area of the gear, of the portion immersed in oil, C_m is the torque load factor, dimensionless. It can be seen from this relationship that the amount of power lost depends on the value of the angular velocity, i.e. on the speed of the driven shaft of the transmission (in the single-gear version). For the C_m factor, numerous experimental studies have been conducted and the following relationship, also due to Changenet et al [94], has been deduced.

$$C_m = \psi_1 \left(\frac{m}{d_2}\right)^{\psi_2} \left(\frac{b}{d_2}\right)^{\psi_3} \left(\frac{h}{d_2}\right)^{\psi_4} \left(\frac{V_0}{d_2^3}\right)^{\psi_5} Re_{b2}^{\psi_6} Fr^{\psi_7} \quad (4.55)$$

where m is the normal module of the gear, d_2 is the pitch diameter of the driven wheel, b is the gear width, h is the immersion depth of the driven wheel in the oil bath, V_0 it is the volume of oil in the sump. It is noted in determining the power factor that its dependency is observed on the geometric characteristics of the gears, or the gear, as well as the volume of oil in the sump (lower half-shell), the value of the Reynolds number, and the Froude number.

Regarding the Re_{b2} number (Reynolds number at the hydraulic radius of the base circle of the driven wheel) and Fr (Froude number), they are determined as follows:

$$Re_{b2} = \frac{V(\frac{d_2}{2})}{\nu} \quad (4.56)$$

$$Fr = \frac{V_0}{\sqrt{g \cdot L_0}} \quad (4.57)$$

V it is the peripheral speed of the driven wheel, d_2 it is the pitch diameter of the driven wheel, ν kinematic viscosity. In the Froude relationship, V_0 is called the reference velocity (peripheral speed), g is the gravitational acceleration, and L_0 is the reference length. In my study, I considered L_0 to be the immersion depth of the driven wheel in the oil sump. Since the Reynolds number and Froude number are dimensionless, the units of measurement can be chosen, but they must be used consistently in the relationship. The Froude number is $Fr=3.56160914$. Values of the factor ψ , and the respective powers ψ^2 - ψ^7 , as shown both in the work [94] and as values taken from the work [97], these values are experimentally determined and strongly dependent on the Reynolds number:

$$\text{For } Re_{b2} < 6000, \quad \psi = (1,366; 0; 0; 0,45; 0,1; -0,21; -0,6) \quad (4.58)$$

$$\text{For } Re_{b2} > 9000, \quad \psi = (3,644; 0; 0,85; 0,1; -0,35; 0; -0,88)$$

It is considered that for Reynolds number values between these limits (6000-9000), the power factor value is taken as the arithmetic mean of the two values determined with the above relations, showing the uncertainty of the theoretical models for determining the power lost by oil churning. In my case, for a chosen oil, H46EP oil, the Reynolds number values reach and slightly exceed 6000.

Regarding the heat exchange surface area, A , I propose the following calculation model, also shown visually in Fig. 4.23.

The oil level expressed in relation to a reference level represented by the tangent to the pitch circle of the driven wheel (in my case d_2) determines two surfaces that will be taken into account when calculating the churning height h . First, the area S_1 is the area (I will also note the area of this area also with S_1) is the area formed by the triangle AOB. The second surface is the surface S (I will also note the area of this surface as S), the area of the sector of the arc circle θ , i.e. the sector OACB. The required area in relation (4.54) is calculated:

$$A = S - S_1 \quad (4.59)$$

where

$$S_1 = \left(\frac{m \cdot z_2}{2}\right)^2 \left(\sin \frac{\theta}{2}\right) \left(\cos \frac{\theta}{2}\right) = \frac{1}{2} (m \cdot z_2)^2 (\sin \theta) \quad (4.60)$$

$$S = \frac{\pi}{4} (m \cdot z_2)^2 \left(\frac{\theta}{180}\right) \quad (4.61)$$

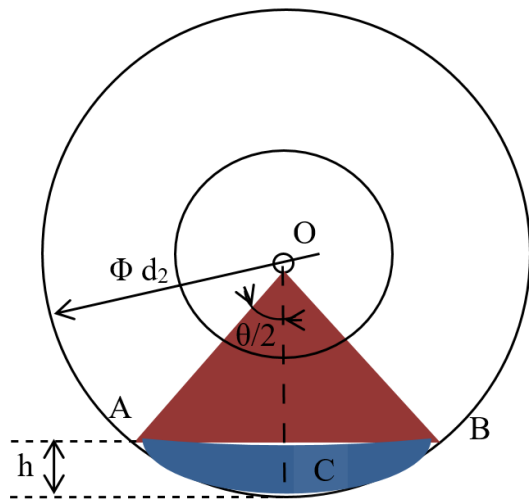


Fig. 4.23. Calculation model

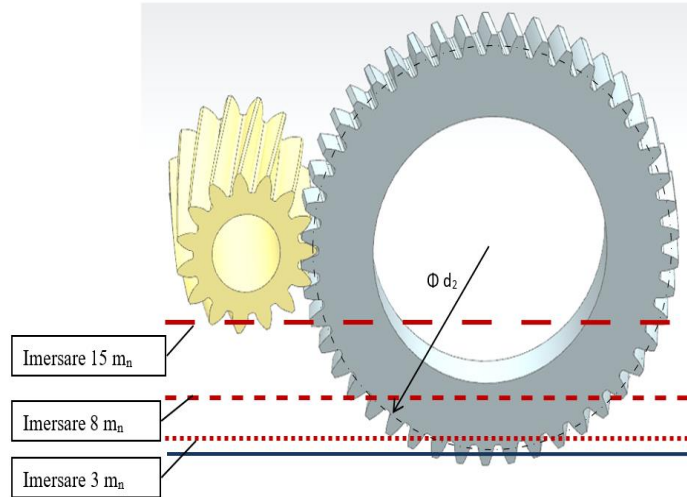
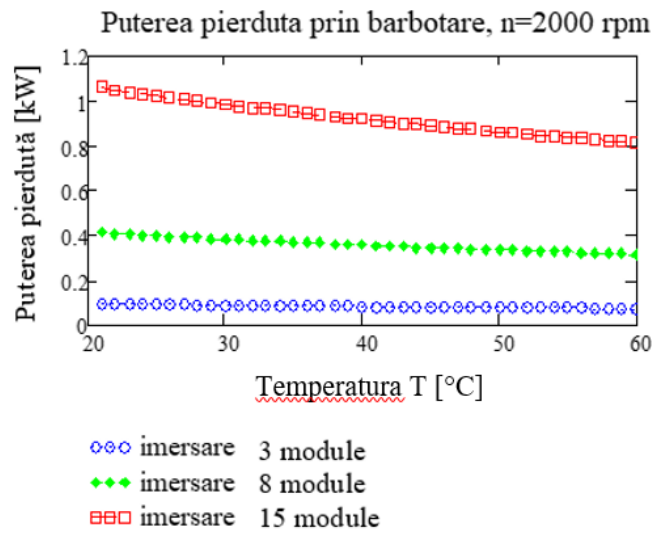
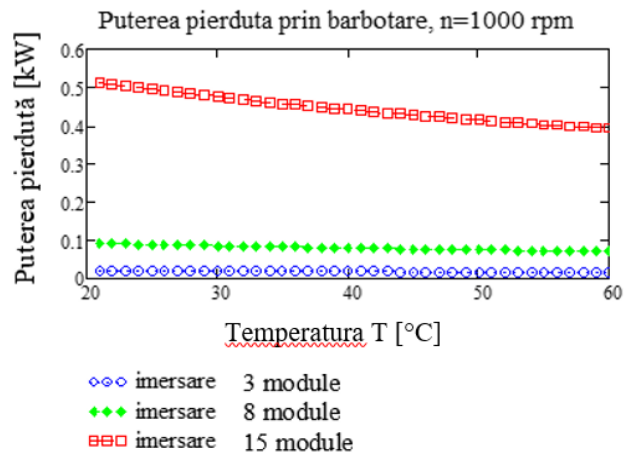


Fig. 4.24. Submersion of the driven wheel in oil



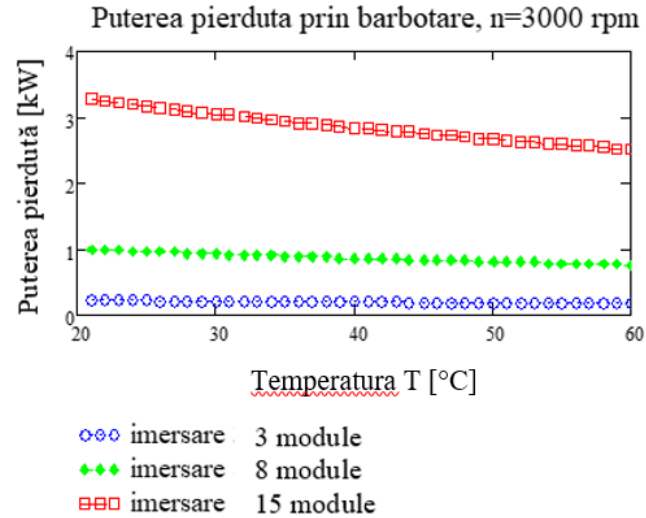


Fig. 4.25. Power loss due to oil churning in P_{VX} (Calculated values)

It is observed that for the analyzed cases, the values of power losses due to oil churning are relatively low, ranging between 0.4...3.5 kW. There is a significant dependence of these losses on the angular velocity magnitude, respectively, the shaft speed with the immersed wheel. Additionally, the dependence of the lost power on the immersion depth of the wheel in the oil sump is noticeable (or the degree of casing oil filling). The power loss increases by more than 3 times when this depth increases fivefold (from the value of three modules, m_n , to the immersion value of 15 m_n).

4.3.6. The total power lost in the transmission

In a gear transmission, the percentage of total power loss can vary between 1...3% depending on the precision and manufacturing technology of the gears, the number of transmission stages, the type of bearings, oil, and seals used, as well as the oil level in which the gears are immersed. Based on the results obtained in the previous subchapters, we have an overview of the total calculated power losses in the considered transmission, a single-stage reduction gearbox with helical gears.

Thus, in Fig. 4.26, the total power lost is observed for a load with a torque $M_t=100$ Nm, at an assumed equilibrium temperature of 60°C, within a range of speeds for which the power loss evaluation was performed individually before. The total value increases from a calculated value of approximately 0.34 kW to a value of about 0.77 kW. The individual contribution of power loss is observed, of which, evidently, the most significant is represented by the gear power loss. The evolution of this loss is linearly increasing with the speed. The same happens with the power loss due to friction, heating in bearings, and seals. The contribution of power losses in seals is comparatively quite small.

Regarding the power loss due to oil churning, it is observed that it is a pseudo-constant, as it is in real-world phenomenology, this loss not being dependent on load and only slightly on speed.

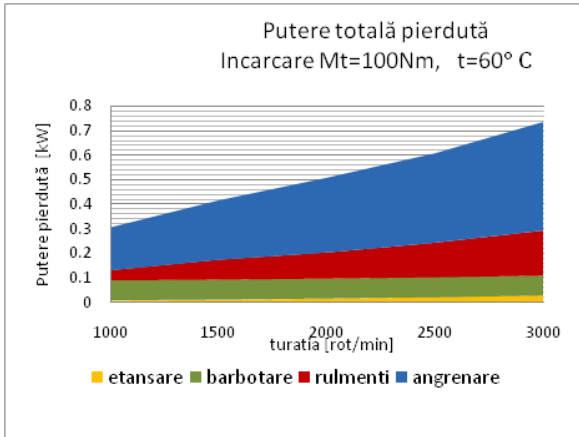


Fig. 4.26. The power loss in different subsystems at the moment of Mt=100 Nm

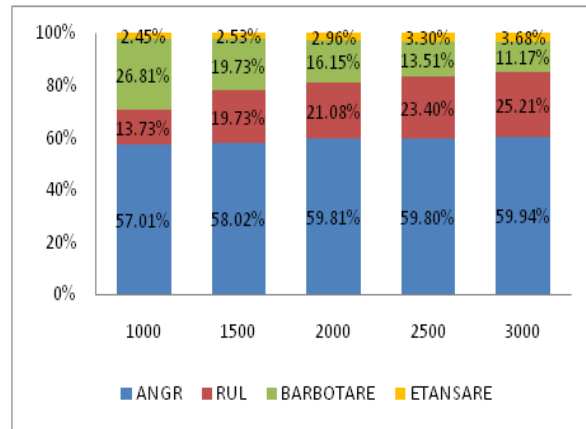


Fig. 4.27. The percentage contribution of power loss, by different sources, at the moment of Mt=100 Nm

For the same data, a statistical analysis was also conducted to highlight the individual contribution of power loss. Thus, it was considered that at each considered speed, there is a lost power that is denoted as 100%, and within this whole, we evaluated the individual percentage losses. This result is presented in Fig. 4.27.

Although it is nearly constant in real values, it is observed that, percentage-wise, the power loss due to oil churning is higher at lower speeds, where the gear power loss is lower (better lubrication conditions with a lower friction coefficient). Similarly, the lubrication conditions of the bearings are better at lower speeds, with the bearings considered partially immersed in the oil bath. Seals, although they also show an increasing trend of power loss with speed, do not contribute significantly to power loss.

The same analysis was performed for the same conditions, at the same speeds but with a load of torque Mt=200 Nm. The results are presented in Figures 4.27 and 4.28, respectively.

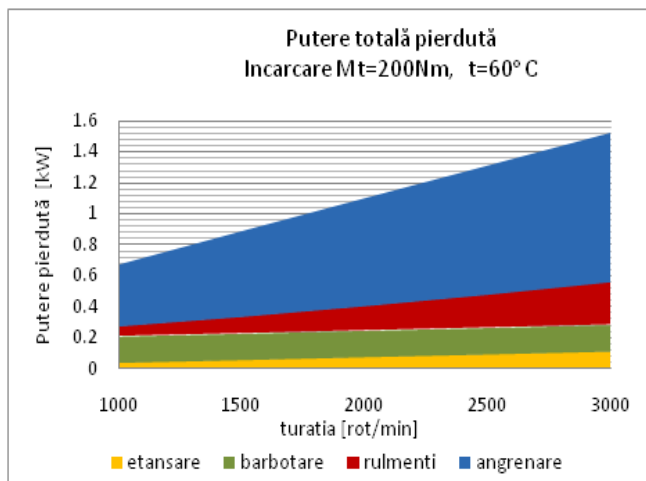


Fig. 4.28. Power loss on the different sources at the moment of Mt=200 Nm (calculated values)

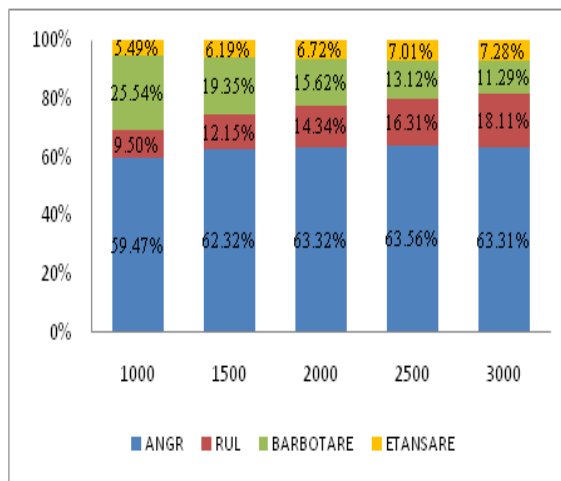


Fig. 4.29. Percentage contribution of power loss on different sources, at the moment Mt=200 Nm (calculated values)

In conclusion, this chapter of the thesis has shown that friction losses in gear meshing are a significant component of power losses in mechanical transmissions, and the friction coefficient varies depending on several factors. Losses increase with speed and load, having a significant impact on transmission efficiency, and must be considered along with other losses to design an optimised transmission.

In total, power losses in a cylindrical gear transmission can range from 1% to 3% of the transmitted power, with a significant impact on transmission efficiency. Minimising these losses is crucial for overall system performance.

Chapter 5. Experimental analysis. Evaluation of power losses in mechanical gear transmissions.

5.1. Introduction

In the experimental part, I will examine in detail the power losses associated with gear meshing, bearings, seals and oil churning in the gearbox. Through these measurements, I aim to identify the main sources of power loss and quantify the contribution of each component to the total power loss in the mechanical gear transmission system.

Before detailing the experiments described in this chapter, a series of earlier tests, mentioned in the previous chapter, were carried out to evaluate the behaviour of mechanical gear transmissions at different speeds, torque levels and three distinct levels of gear immersion in oil. These tests involved shorter test periods, 40 minutes for the load tests and 80 minutes for the churning tests, compared to the actual experiments, which have a significantly longer duration of about 4-5 hours until equilibrium temperature is reached.

The difference in the duration of previous and current tests reflects the increased emphasis on investigation under prolonged operating conditions in the current study. The earlier tests, although shorter, played a crucial role in establishing the foundations of my research and defining the essential parameters for the more complex and extensive experiments presented in this stage of the thesis. Thus, this transition from shorter tests to longer experiments represents a significant evolution in our experimental approach, ensuring the accuracy and relevance of the data collected in investigating power losses in mechanical transmissions.

5.2. Test rig presentation

In order to validate the data presented in the previous chapters, we used the gear testing and lubricant testing rig located at INCDT Comoti.

The gear testing and lubricant testing rig is a closed loop test rig designed to provide torque between 0 - 200 Nm and speed between 0 - 3200 rpm. This test rig is equipped with the following components:

- Optical transducers, 2 units, type ROC 425, manufactured by Heidenhain of Germany,
- T10FS non-contact flange type torque transducer, from Hottinger Baldwin Messtechnik, with an accuracy class of 0.05%,
- PT100 bath oil temperature transducers,
- vibration measurement sensors on the test stand, Bently Nevada,
- two gearboxes, one for test and one for return,
- Bently Nevada electric motor vibration measurement sensors.

The data obtained from this test stand formed the basis for the validation and interpretation of the results obtained in the previous chapters of this PhD thesis.

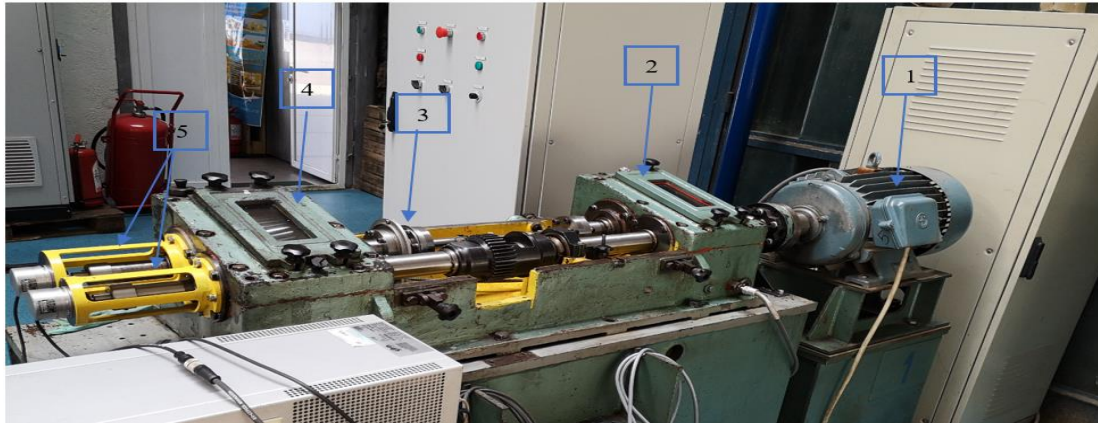


Figura 5.1. The testing rig for gears and lubricants

1- electric motor; 2- return transmission; 3- torque transducer T10FS; 4- test transmission; 5- optical transducers type ROC 425

Table 5.1 Geometry and characteristics of the gear test rig (see also Chapter 2)

Characteristics	Notation	Value	Characteristics	Notation	Value
Axis distance [mm]	a_w	125	Hardness of the pinion	HB	270-290
Number of teeth for pinion	z_1	15	Hardness of the wheel	HB	290-310
Number of teeth for wheel	z_2	46	Tooth flank roughness	R_a	0.4
Helix angle [°]	β	10	Type of bearings	-	21310E
Displacement coefficient for pinion	x_1	0.427	Distance between bearings	-	200
Displacement coefficient for wheel	x_2	-0.138	Type of oil	-	H46EP
Pinion width [mm]	b_1	80,37	Oil volume [l]	V_{oil}	5.3
Wheel width [mm]	b_2	73,37	Oil density [kg/m ³]	ρ	877
Gear coverage ratio	ε_a	1.4523	Average oil heat capacity	C_p	2.121
Additional gear coverage ratio	ε_β	1.013			
Precision class	-	6			
Material	-	41MoCr11			

Additional tooth coverage, $\varepsilon_\beta = 1,013$ allowed for the reduction of vibration levels.

The initial validation procedure of the experimental setup was crucial in ensuring the proper functioning of each component and validating the integrity of experimental data. Checks included a careful examination of the non-contact torque transducer, precise addition of H46EP

oil, and a detailed analysis of the control panel. These operations were essential to guarantee the reliability and accuracy of the results obtained in the research on power losses in mechanical transmissions with gears.

For the validation of the theoretical data presented in the previous chapters, the following tests were conducted on the gear testing and lubricant testing rig within the INCDT COMOTI facility:

T1 - Churning test with torque $M_t=0$ Nm and speed $n=1500$ rpm,

T2 - Churning test with torque $M_t=0$ Nm and speed $n=2000$ rpm,

T3 - Churning test with torque $M_t=0$ Nm and speed $n=3000$ rpm,

T4 - Load test with torque $M_t=150$ Nm and speed $n=1500$ rpm, Calculated Power=23.562 kW,

T5 - Load test with torque $M_t=150$ Nm and speed $n=2000$ rpm, Calculated Power=31.416 kW,

T6 - Load test with torque $M_t=200$ Nm and speed $n=1500$ rpm, Calculated Power=31.416 kW,

T7 - Load test with torque $M_t=200$ Nm and speed $n=2000$ rpm, Calculated Power=41.888 kW,

where

T1...T7 is the test number,

M_t - Torque [Nm],

n - Speed [rpm],

$P_{\text{calculated}}$ - Calculated input power [kW].

These tests were designed to cover a wide range of operating scenarios, providing essential data for the analysis of power losses in gear transmissions.

5.3. Testing procedure

Testing procedure is a crucial stage in the investigation of power losses in mechanical transmissions with gears. By implementing a rigorous set of operations, this stage aims to obtain the necessary data for evaluating the complex phenomena within transmission systems.

Firstly, the control panel and data collection system are started, marking the beginning of the testing experience. Before loading the system with the desired torque, the stand's condition is checked, and the temperature of the test box's oil bath is measured. The values of ambient and oil temperatures are carefully recorded.

Calibrating the torque transducer is essential to ensure measurement accuracy. Loading the system with the desired torque is done carefully, using a spline key, while setting the required speed, and starting the timer to monitor the system's evolution over time.

Periodically, the time and temperature values in the test box's oil bath are noted, providing a detailed picture of thermal changes during the tests. At the end of the experiment, the process is stopped, and the inspection cover of the test box is opened to take thermal images of the gear teeth (Fig. 5.3.), bearings (Fig. 5.4.), and test box housing (Fig. 5.5.) using the Fluke TiS60+ thermal imaging camera.

It is important to note that we chose to use H46EP oil in the test box, with a gear immersion level of 8 modules. The return box also uses H46EP oil, with the same gear immersion level. The oil volumes corresponding to the 8-module gear immersion level are 5.3 liters in the test box and, respectively, in the return box. Precise measurements of oil temperature are obtained using PT100 sensors in the oil baths, and the Fluke thermal imaging camera provides essential thermal images of gears, bearings, and the test box housing after each test.

This detailed testing procedure forms the foundation upon which I relied to obtain authentic and relevant data in the comprehensive exploration of power losses in mechanical transmissions with gears.

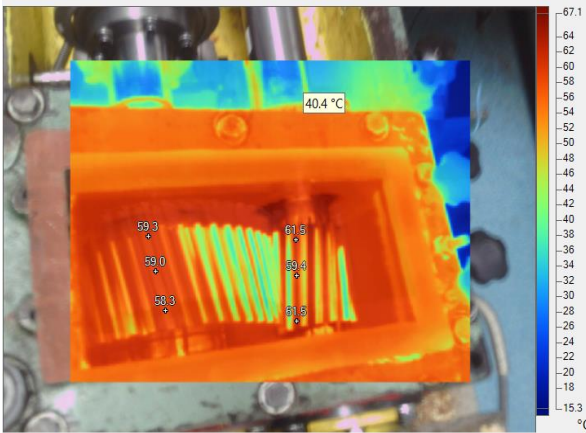


Fig. 5.3. The gear temperature after the churning test, at $n=3000$ rpm

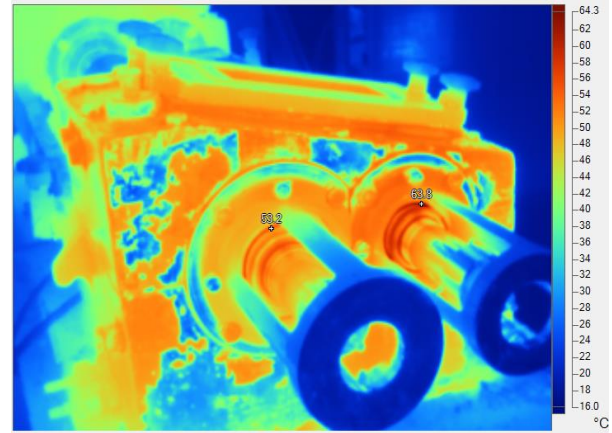


Fig. 5.4. The bearing temperature after completing the 200 Nm load test at 2000 rpm

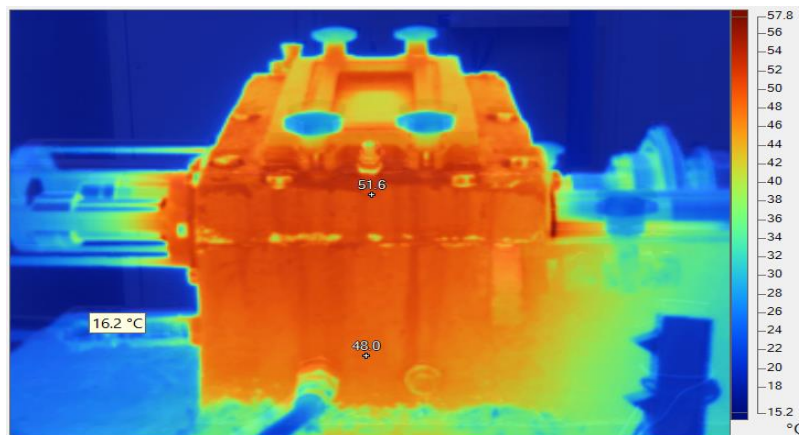


Fig. 5.5. The temperature of the test case after completing the 200 Nm load test at 2000 rpm

5.4. Results of the tests

This section represents a crucial step in understanding the thermal behavior of the mechanical transmission, focusing on the results obtained from a series of detailed tests. The main purpose of these tests was to investigate the distribution and variations of temperature in various operating scenarios of the transmission. By recording temperatures in the oil bath and on the system casing, I aimed to highlight how critical factors such as speed and loading interact concerning the thermal performance of this vital component of transmission mechanisms.

Moreover, within these tests, I assessed the power lost in the system using both experimental methods and theoretical calculations. The comparison between experimentally determined power loss and theoretically calculated power loss provides a broader perspective on thermal performance, highlighting potential discrepancies and offering insights into the mechanisms influencing the efficiency of the mechanical transmission. The detailed presentation of results, including power losses and collected thermal data, will allow us to draw meaningful conclusions regarding the thermal performance of this mechanical transmission under various operating conditions.

All the test results with the immersion of the driven wheel by 8 normal modules (32 mm) have been compiled in Table 5.2.

Table 5.2 Tests with the immersion of the wheel by 8-normal modules

Wheel Immersion Tests with 8 m _n							Final casing temperature	
Test no.	Moment M _t [Nm]	Rotation Speed n [rpm]	Ambient temperature [°C]	Final oil temperature [°C]	Calculated lost power [W]	Lost power, experimentally determined [W]	A [°C]	B [°C]
T1	0	1500	13,5	35,5	161	156	30,5	33,5
T2	0	2000	14,7	40,5	197	190	35	38,5
T3	0	3000	16	58,5	371	359	51	54
T4	150	1500	16,2	43	213	199	39	42
T5	150	2000	16,5	50,5	289	269	46	49
T6	200	1500	18,8	48,1	240	223	44,5	47
T7	200	2000	15	54,5	357	326	48	52

The experimental power loss was determined using the method presented in subsection 5.5, i.e., using the calculation expression (5.2).

In Table 5.3 and, respectively, Fig. 5.6, the temperatures in the oil bath and on the test housing are highlighted for the 3 churning tests, T1, T2, and T3, at 1500 rpm, 2000 rpm, and, respectively, 3000 rpm, with the oil level at 8 module immersion depth for the wheel.

Table 5.3. Oil churning at a level of immersion of the driven wheel by 8 normal modules

Churning at 8 normal module level					
Test no.	Rotation speed	Ambient temperature [°C]	Final oil temperature [°C]	Casing temperature A [°C]	Casing temperature B [°C]
T1	n=1500	13,5	35,5	30,5	33,5
T2	n=2000	14,7	40,5	35	38,5
T3	n=3000	16	58,5	51	54

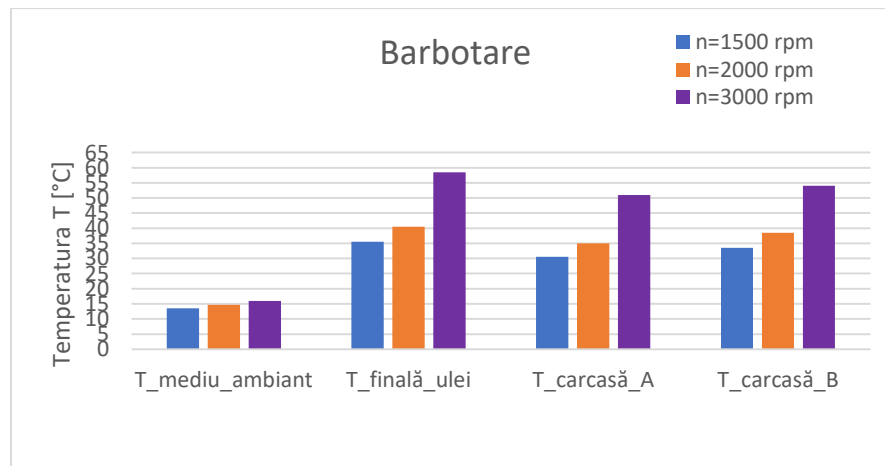


Fig. 5.6. Temperature measurement results for churning tests

The figures and tables above for the churning tests indicate that the temperature in the oil bath and on the casing increases with the speed. The final oil outlet temperatures increase with the speed, ranging from 35.5 °C to 58.5 °C.

Table 5.4. Tests with a load of $M_t=150$ Nm, with the immersion level of the driven wheel at 8 normal modules

Test no. / speed n [rpm]	$M_t=150$ Nm with oil level at $8 m_n$			
	Ambient temperature [°C]	Final oil temperature [°C]	Casing temperature A [°C]	Casing temperature B [°C]
T4 / n=1500	16,2	43	39	42
T5 / n= 2000	16,5	50,5	46	49

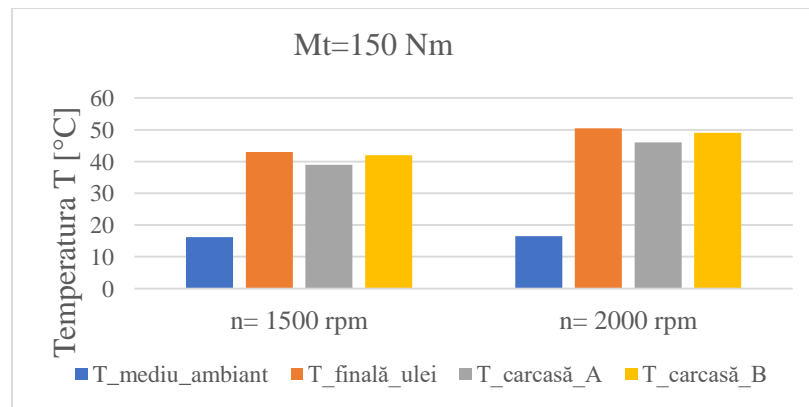


Fig. 5.7. Temperatures recorded at the end of the tests with a load of $M_t=150$ Nm

In Table 5.4 and Figure 5.7, the temperatures in the oil bath and on the housing for the two load tests with $M_t=150$ Nm, T4 and T5, at 1500 and 2000 rpm, respectively, are highlighted at the 8-module immersion level of the driven wheel.

The minimum final oil temperature is at 1500 rpm with a value of 43°C, and the maximum is 50.5°C at 2000 rpm.

Table 5.5. Results obtained from tests with a load of $M_t=200$ Nm, with the immersion level of the driven wheel at 8 normal modules

Test no. / speed n [rpm]	$M_t=200$ Nm with oil level at $8 m_n$			
	Ambient temperature [°C]	Final oil temperature [°C]	Casing temperature A [°C]	Casing temperature B [°C]
T6 / n=1500	18,8	48,1	44,5	47
T7 / n=2000	15	54,5	48	52

In Table 5.5 and Figure 5.8, the temperatures in the oil bath and on the housing are highlighted for the two load tests with $M_t=200$ Nm, T6 and T7, at 1500 rpm and 2000 rpm, respectively, with an oil immersion level of 8 normal modules for the driven wheel.

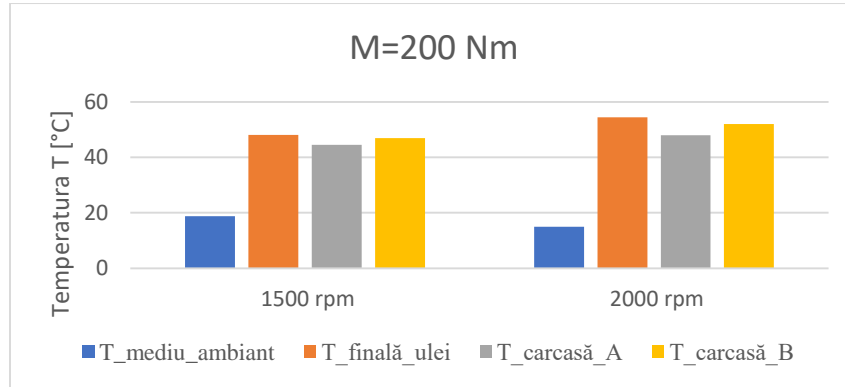


Fig. 5.8. Results of temperature measurements for tests with $M_t=200$ Nm, with an immersion level of 8 normal modules for the driven wheel

The minimum final oil temperature is at the 1500 rpm test, reaching 48.1°C and increasing to approximately 54.5°C at the 2000 rpm test.

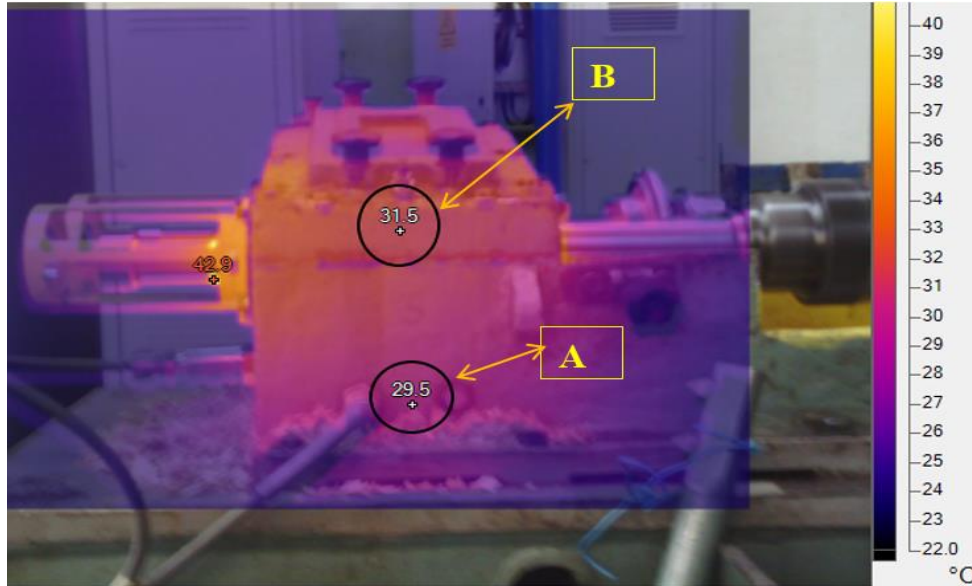


Fig. 5.9. Final temperatures of the semi-casings at points A and B

In Figure 5.9, points A and B on the lower semi-casing and upper semi-casing, respectively, are marked, where temperatures were measured after each test, and they are found in the tables with the test results.

These tables and figures, together, contribute to understanding how different levels of load and speed influence the thermal behavior of the mechanical transmission, providing concrete data and graphical illustrations that help outline conclusions relevant to the system's performance and efficiency.

In this chapter, we addressed the experimental part of the research on power losses in mechanical transmissions with gears. Our goal was to obtain concrete data and relevant measurements to assess and understand the power loss phenomena within gear transmission systems. For this purpose, we designed and conducted rigorous tests with different torque and

speed levels to cover various operating scenarios on a specialized testing rig equipped with high-precision components.

The main results obtained in the experimental part are as follows:

1. The temperature dependency in relation to speed. I observed that temperatures, both in the oil bath and on the transmission casing, increase with the rise in speed. This increase is attributed to the complex interactions among gears, bearings, and lubricating oil during operation at high speeds.
2. The impact of meshing torque. I noted that power losses have a direct dependence on torque. The higher the transmitted torque, the more power losses increase proportionally.
3. Thermal analysis of components. Using the Fluke thermal imaging camera, I obtained thermal images of the gear teeth, bearings, and transmission casing. These images once again confirmed that power losses are associated with an increase in temperature in critical areas of the transmission.

The experimental data obtained are essential for validating the theoretical results presented in the previous chapters of this doctoral thesis.

This experimental approach has allowed the identification of the main causes of power losses and the generation of a set of authentic and well-founded data. Using the results presented in Chapter 5.5, the obtained equilibrium temperatures allow for the determination of the total power losses in the studied test gearbox.

In conclusion, the experimental part of this doctoral thesis has made a valuable contribution to understanding and improving mechanical transmissions with gear wheels. The data obtained through rigorous testing have provided new information and validated important theoretical aspects.

5.5. Establishing the dependence of power dissipated through the housing on the temperature difference between the oil bath and the ambient environment.

This subsection presents an analysis of the heat transfer capacity and power losses in a mechanical transmission with helical gears, as well as in a transmission on an FZG-type test rig. The purpose of the tests was to establish a correlation between the thermal power dissipated through the transmission housing and the temperature difference between the oil in the bath and the ambient environment. This was achieved by heating the bath oil using electric resistors and inducing mild agitation through the rotation of the gear without a load.

Experiments were conducted using a gear and lubricant testing system equipped with a closed-loop circuit and measurement instruments. Calibrated electric resistors were employed to heat the oil in the test rig. The electric current through the resistors was adjusted using a voltage variator to achieve different constant levels of thermal power, maintaining a constant power level until the equilibrium temperature corresponding to each adjusted power level was reached. The obtained equilibrium temperatures are listed in Table 5.6. This study provides insights into the heating process of the test rig in the transmission housing area, implicitly addressing power losses in a gear system. Such information can be valuable in the design and optimization of mechanical transmissions with gears. The procedure can be applied in situ for the experimental determination of the thermal power dissipated through the housing of a gear transmission.

In this study, the testing rig for gears and lubricants presented in Figure 5.11 was employed to conduct the experiments.

The following auxiliary components were used for test validation: a voltage variator, a socket with a digital energy meter monitoring instantaneous power, 2 electric resistors of 400 W each (maximum), and a Fluke TiS60+ thermal camera.

The obtained results not only reveal the thermal behavior of the components but also provide valuable information for optimization and innovation in mechanical transmission design. Furthermore, this testing methodology can serve as an essential tool for the experimental assessment of the thermal power dissipated through the gearbox housings.



Fig. 5.11. The testing rig for gears and lubricants equipped with electric resistors, a socket with a digital energy meter, and a voltage variator

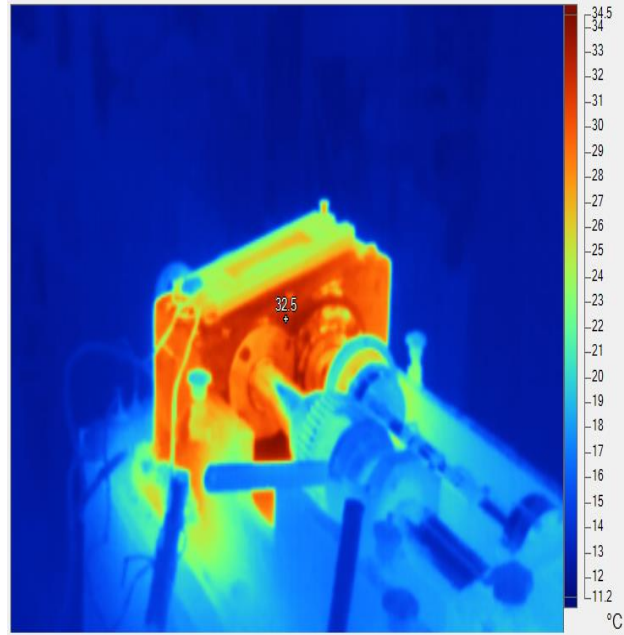


Fig. 5.13. The infrared image of the test case during the ongoing test T7R, with a thermal power of 750 W

In Figure 5.13, the temperature distribution in various zones of the casing is observed.

The differential equation of the heating process of the test rig is as follows:

$$m_{ech} \cdot c_{ech} \cdot dT = [P - A_{ech} \cdot k_{ech} \cdot (T - T_0)] \cdot dt \quad (5.1)$$

where

$m_{ech} \cdot c_{ech}$ represents the equivalent capacity of thermal energy storage in the test rig.

$dQ = m_{ech} \cdot c_{ech} \cdot dT$ is the variation of thermal energy accumulated in the test rig during dt .

P it is the thermal power (heat flux) received by the system. If we use an electric resistor as a thermal source to simulate the heating of the test rig, the power P is constant.

$A_{ech} \cdot k_{ech}$ it is the characteristic of the test rig to dissipate heat into the surrounding environment. Due to the thermal gradient within the rig, dissipation is non-uniform, as is the heat storage within the rig.

$A_{ech} \cdot k_{ech} \cdot (T - T_0)$ it is the thermal power dissipated into the ambient environment. Initially, $T = T_0$ and all the thermal power enters the stand, heating it. When the equilibrium temperature

Tequilibrium is reached, no more thermal energy is accumulated in the stand, and practically all the generated thermal power is dissipated into the environment.

In the differential equation, it can be observed that if the temperature measured in the oil bath in the casing stabilizes, i.e., dT becomes equal to 0, only the right-hand side of the equation remains, allowing the establishment of a relationship between the thermal power inside the reducer and the temperature difference, $T_{echilibru} - T_0$, between the temperature measured in the oil bath and the ambient temperature.

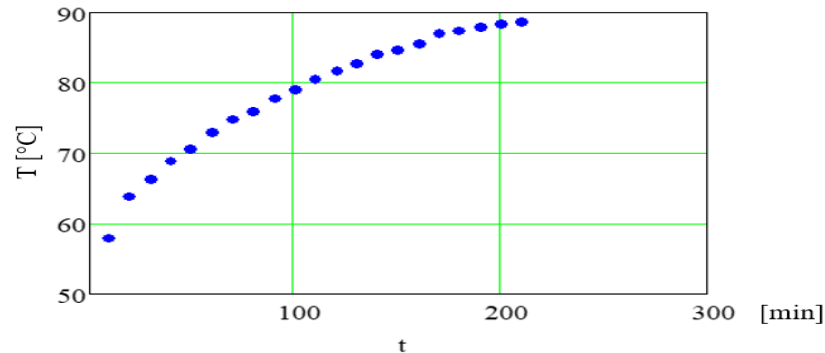


Fig. 5.14 The values of the oil temperature in the oil bath, for $P=750$ W:
($T_{mediu} = 15,5^\circ\text{C}$, $T_{echilibru} = 88,7^\circ\text{C}$)

In the graph in Figure 5.14, it can be observed that, over time, the oil bath temperature stabilizes, resulting in an equilibrium temperature ($T_{echilibru}$), used to establish the correlation between the thermal power released by the electric resistors and the temperature difference between the temperature $T_{echilibru}$, measured in the oil bath and the temperature T_0 , equal, in this case, to 15.5°C , that is $\Delta T = 88,7 - 15,5 = 73,2^\circ\text{C}$.

Seven tests were conducted with seven different power levels, and equilibrium temperatures were obtained in the test rig. At this point, the entire thermal power is dissipated through the casing, and its temperature no longer increases, as shown in Figure 5.14.

The tests were conducted on different days and had different ambient temperatures. To determine the oil temperature in the casing as accurately as possible, the oil agitation was simulated by manually aerating it with the driven wheel. The test results using electric resistors are summarized in Table 5.6.

Table 5.6. Compiling the results of tests with electric resistors

Test no.	Ambient temperature, T_0 [$^\circ\text{C}$]	Power [W]	Equilibrium temperature $T_{echilibru}$ [$^\circ\text{C}$]	ΔT [$^\circ\text{C}$]
T1R	14	85	27	13
T2R	14	185	39,5	25
T3R	15,5	310	54	38,5
T4R	14,5	390	59	44,5
T5R	16	430	65	49
T6R	16	570	77	61
T7R	15,5	750	88,7	73,2

The correlation of power with the temperature difference between the oil and the ambient temperature from Table 5.6 was approximated with the following polynomial, whose coefficients were determined through regression:

$$P(\Delta T) = 5.234970817136151 \cdot \Delta T + 0.0925589083718236 \cdot \Delta T^2 - 0.0004028413613011809 \cdot \Delta T^3 \quad (5.2)$$

In the graph from Fig. 5.15, the measured values are compared with those calculated using the polynomial (5.2). It is noted that the maximum relative deviation is 2.43%.

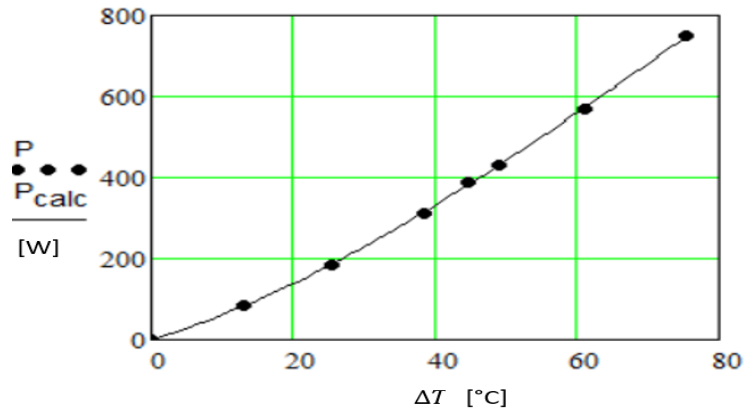


Fig. 5.15. The measured values and those calculated with the polynomial (5.2) for the tests with electric resistors

From the graph in figure 5.15, a good agreement between the calculated and measured values can be observed.

The next step involves using the difference between the equilibrium temperature in the oil bath and the ambient temperature, ΔT , to determine the value of the thermal power P_V , released at the established equilibrium temperatures (as in Figure 5.14), in the case of oil churning experiments (with the unloaded test rig) and those conducted with the loaded test rig, presented in subchapter 5.4, in table 5.2. These values allowed for a comparison with the results of theoretical calculations.

The conclusions of this highly complex and rigorous study, conducted within the doctoral thesis, successfully demonstrate a new innovative approach in analyzing the heat transfer capacity and power losses in mechanical transmissions with helical gears. The primary objective of these tests was to establish a robust and accurate correlation between the thermal power dissipated through the transmission housing and the temperature difference between the oil bath and the ambient environment.

The method used in this chapter can be employed in situ for the experimental study of the actual thermal behavior of enclosed mechanical transmissions, specifically those with gears.

With advanced testing methods and sophisticated instruments, remarkable results have been achieved based on the differential equation (5.1) for the stand's heating process. A good agreement between the measured values and those calculated using the polynomial (5.2) has been highlighted. This attests to the quality and high precision of these experimental determinations.

The study has benefited from a holistic and comprehensive approach, covering essential aspects related to the thermal behavior of the gearbox, including power losses in the gear system. The conclusions and results obtained will serve as a solid foundation for the optimization and

further design of similar systems, thereby contributing to the improvement of their efficiency and performance.

The results of this study have made a significant contribution to the field of thermal research in gears, opening new horizons for researchers and engineers in this area. The methods and technologies developed in this research project will be valuable for the scientific community and industry, with the potential to significantly improve the performance and durability of mechanical transmission systems.

In conclusion, this study represents a notable contribution to the advancement of scientific knowledge in the field of mechanical transmissions and heat transfer, bringing significant benefits to technological development and enhancing energy efficiency in various industrial applications. Further exploration of these results and the pursuit of new research directions may lead to substantial progress in the field, solidifying this doctoral thesis as a valuable and reference contribution in scientific research.

Chapter 6. Final conclusions and main contributions to power losses analysis in a thermal network with mechanical transmission and the experimental part: assessment of power losses in gear mechanisms

6.1. General conclusions

(1) From the analysis of the current state of experimental studies on helical gears, important conclusions have emerged, presented in Chapter 2. These conclusions have provided insight into the current state of helical gears, identifying key aspects that require further research and improvement.

(2) Given the data and conclusions from the analysis of the current state of experimental studies on helical gears, the research and development directions presented in § 3.1 were considered to be relevant. These directions formed the basis for planning further research and development, ensuring a focus on relevant and promising aspects.

(3) In relation to the current state and research and development directions regarding the analysis of power losses in a thermal network with mechanical transmission, the main objective of the research and development activities within the doctoral program (see also § 3.2) was determined to establish and validate innovative solutions for the theoretical and experimental analysis of power losses in mechanical transmissions.

(4) The relevant conclusions regarding the doctoral research and development activities to achieve its main objective, in relation to the methodological reference elements (see § 4.3), are as follows:

- identified and quantified the main sources of power loss in gear transmissions, providing essential information for optimizing existing systems and developing new technologies,
- conducted tests and measurements in the experimental part to assess and understand power loss phenomena in gear transmissions, contributing to the development of efficient and durable solutions,
- proposed and tested an innovative method for the experimental determination of power losses in a gear transmission, based on the temperature difference between the oil bath and the ambient environment, correlating it with the thermal power dissipated in the ambient environment established using calibrated electric resistors, as presented in

subchapter 5.5. The method is applicable in situ for gear transmissions in sealed housings with gear lubrication by immersion.

(5) In achieving the main objective of the doctoral research and development activity, the present doctoral thesis brings several contributions, among which the most important are as follows:

- developing an advanced mathematical model for the analysis and simulation of the behavior of gear transmissions in thermal networks, providing a valuable tool for the design and optimization of systems,
- identification and critical evaluation of factors influencing power losses in thermal networks, contributing to the development of effective reduction strategies,
- development of innovative methods and techniques for measuring and monitoring power losses in mechanical transmissions (see the method in subsection 5.5), facilitating the implementation of predictive maintenance solutions.
- innovative experimental procedure for determining power losses in mechanical transmissions was developed, tested, and utilized, applicable in-situ across various industrial applications.

The present doctoral thesis, through its problem statement, approach, and results, provides a profound understanding of power losses in a thermal network with mechanical transmission and makes significant contributions to both theoretical and experimental analyses in this field. The scientific importance of the thesis is underscored by advancing knowledge in this domain and developing innovative solutions. Simultaneously, its practical significance lies in the applicability of the results and the positive impact on both the industry and the specialist community.

6.2. Original contributions of the doctoral thesis

Considering the results obtained in these chapters, the following contributions can be identified:

Theoretical contributions:

1. Analysis of the history and evolution of gear wheels, providing a historical perspective on the development of these critical mechanical components.
2. Investigation and presentation of gear testing rigs, including their types and the current state of experimental research in the field of gears.

Modeling-simulation contributions:

3. Development of 2D and 3D numerical models for external cylindrical gears with inclined involute profiles using numerical methods and specialized software such as Siemens Unigraphics NX 12 and Solid Edge ST9. These models were manufactured at mechanical factory Cugir S.A. and utilized on the testing rig within the INCDT COMOTI facility.
4. Detailed comparison of involute profiles generated in Siemens Unigraphics NX and Solid Edge, providing a critical evaluation of these modeling methods.
5. Presentation of relevant conclusions regarding the differences and similarities between the models generated in NX and SE, including aspects related to the use of libraries for modeling.
6. The numerical calculation of power losses in a helical gear mechanical transmission, accomplished through 6 codes written in Mathcad.

Methodological contributions:

7. The necessary parameters were defined in the development of a research methodology for assessing power losses in a mechanical transmission with cylindrical gear teeth and inclined teeth..
8. Defining the main objectives of research and development activities and establishing research directions to effectively address these objective.

Experimental contributions:

9. Conducting an experimental study on power losses in a mechanical transmission with gears.
10. Instrumentation of the testing rig used for assessing power losses in mechanical transmissions with gears.
11. Equipping the testing rig with auxiliary instruments for tests involving electric resistors and establishing the testing procedure used.
12. Establishing the dependence of power dissipated through the transmission casing on the temperature difference between the oil bath and the ambient environment, simulating the heating of the rig with electric resistors of various thermal powers.
13. Analyzing the results of churning lubrication and under load tests, as well as experimentally determining the power dissipated through the transmission casing based on the temperature difference between the oil bath and the ambient environment.

Selective bibliography

- [1] Gopinath, K., & Mayurat, M. M. *Lecture 1: Introduction to Gears - Machine Design II Module 2*. https://www.academia.edu/7694046/Machine_Design_II_Module_2_-GEARS_Lecture_1_-INTRODUCTION_Contents.
- [2] *An ancient Greek computer*. (1959). *Scientific American*, 200(6), 60-67. https://en.wikipedia.org/wiki/Antikythera_mechanism.
- [5] *South-pointing chariot*. (2018). *Wikipedia*: https://en.wikipedia.org/wiki/South-pointing_chariot.
- [7] Istituto e Museo di Storia della Scienza. (2004). *Codex Atlanticus (BAM), fol. 1103r (detail)*. <https://brunelleschi.imss.fi.it/genscheda.asp?appl=LIR&xsl=paginamanoscritto&lingua=ENG&chiave=100821>.
- [8] Newtown_graffiti. (2010). *Graffiti Art*. Flickr. https://www.flickr.com/photos/newtown_graffiti/4803665199.
- [11] Burrows, M., & Sutton, G. (2013). Interacting gears synchronize propulsive leg movements in a jumping insect. *Science*. <https://www.cam.ac.uk/research/news/functioning-mechanical-gears-seen-in-nature-for-the-first-time>.
- [12] Chironis, N. P. (1967). *Gear Design and Application*. McGraw-Hill Book Co.
- [13] Hargreaves, D. J., & Planitz, A. (2009). Assessing the energy efficiency of gear oils via the FZG test machine. *Tribology International*, 42, 918-925. Elsevier.
- [14] Li, S. (2008). Contact problem and numeric method of a planetary drive with small teeth number difference. *Mechanism and Machine Theory*, 43.
- [15] Gabroveanu, I. S., Tudor, A., Mirica, R., & Cananau, S. (2016). FEM analysis of gear width influence on the mesh stiffness at helical gears. *Scientific Bulletin, series D, Universitatea Politehnica din Bucuresti*.

- [16] Davali, P., Rosa, F., Rossi, F., & Boni, G. (2007). Transmission error and noise emission of spur gears. *Geartechnology*, 78.
- [17] Raja Hamzah, R. I., & Mba, D. (2007). The influence of operating condition on acoustic emission (AE) generation during meshing of helical and spur gears. *Tribology International*, 42, 3-14. Elsevier.
- [18] Tan, C. K., & Mba, D. (2004). Identification of the acoustic emission source during a comparative study on diagnosis of a spur gearbox. *Tribology International*, 38, 469-480.
- [19] Nguyen, V. K., Cau, T. M., & Dien, N. P. (2004). Modelling Parametric Vibration of Gear-Pair Systems as a Tool for Aiding Gear Fault Diagnosis. *Technische Mechanik*, 24(3-4).
- [33] Rădulescu, Gh., Miloiu, Gh., Gheorghii, N., & Muntean, C. (1986). Indrumar de proiectare in constructia de masini, Vol. III. *Editura Tehnica*, Bucuresti.
- [56] Niemann, G., & Winter, H. (2003). *Maschinenelemente Band 2*. Springer Verlag, 2. Auflage, pp. 243-257.
- [57] Höhn, B.-R., Michaelis, K., & Hinterstoißer, M. (2009). Optimization of gearbox efficiency. *Gorivaimaziva*, 48(4), 462–480.
- [60] Fernandes, C. M. C. G., Marques, P. M. T., Martins, R. C., & Seabra, J. H. O. (2015). Influence of gear loss factor on the power loss prediction. *Mech. Sci.*, 6, 81–88. <https://doi.org/10.5194/ms-6-81-2015>.
- [71] Castro, J., & Seabra, J. (1998). Scuffing and lubricant film breakdown in FZG gears part I: Analytical and experimental approach. *Wear*, 215(1), 104–113.
- [89] SKF. (November 2005). *SKF General Catalogue 6000 EN*.
- [90] Standuri pentru testarea transmisiilor cu roti dintate. (n.d.). *Tehnica și Tehnologie Online*. Retrieved from <https://www.ttonline.ro/revista/transmisii-mecanice/standuri-pentru-testarea-transmisiilor-cu-roti-dintate>.
- [91] Jelaska, D. (2012). *Gears and gear drives* (Chapters 2, 3, and 4). John Wiley & Sons, Ltd.
- [94] Changenet, C., & Vex, P. (2007). A model for the prediction of churning losses in geared transmissions—preliminary results. *Journal of Mechanical Design*, 129(1), 128.
- [97] Prakash Del Valle, C. (2014). *Thermal modelling of an FZG test gearbox* (Master's thesis). KTH Industrial Engineering and Management, Machine Design.